

ORIGINAL RESEARCH ARTICLE



Long Noncoding RNA *MIAT* Controls Advanced Atherosclerotic Lesion Formation and Plaque Destabilization

Francesca Fasolo, PhD*¹; Hong Jin¹, MD, PhD*¹; Greg Winski¹, MD*¹; Ekaterina Chernogubova, PhD¹; Jessica Pauli¹, MSc¹; Hanna Winter¹, MSc¹; Daniel Y. Li, MD, PhD¹; Nadiya Glukha, MSc¹; Sabine Bauer¹, MSc¹; Susanne Metschl, DVM¹; Zhiyuan Wu, MD¹; Marlys L. Koschinsky, PhD¹; Muredach Reilly¹, MBBCh, MSCE¹; Jaroslav Pelisek, PhD¹; Wolfgang Kempf, PhD¹; Hans-Henning Eckstein¹, MD¹; Oliver Soehnlein¹, MD, PhD¹; Ljubica Matic¹, PhD¹; Ulf Hedin¹, MD, PhD¹; Alexandra Bäcklund, PhD¹; Claes Bergmark, MD¹; Valentina Paloschi¹, PhD†¹; Lars Maegdefessel¹, MD, PhD†¹

BACKGROUND: Long noncoding RNAs (lncRNAs) are important regulators of biological processes involved in vascular tissue homeostasis and disease development. The present study assessed the functional contribution of the lncRNA myocardial infarction-associated transcript (*MIAT*) to atherosclerosis and carotid artery disease.

METHODS: We profiled differences in RNA transcript expression in patients with advanced carotid artery atherosclerotic lesions from the Biobank of Karolinska Endarterectomies. The lncRNA *MIAT* was identified as the most upregulated noncoding RNA transcript in carotid plaques compared with nonatherosclerotic control arteries, which was confirmed by quantitative real-time polymerase chain reaction and in situ hybridization.

RESULTS: Experimental knockdown of *MIAT*, using site-specific antisense oligonucleotides (LNA-GapmeRs) not only markedly decreased proliferation and migration rates of cultured human carotid artery smooth muscle cells (SMCs) but also increased their apoptosis. *MIAT* mechanistically regulated SMC proliferation through the EGR1 (Early Growth Response 1)-ELK1 (ETS Transcription Factor ELK1)-ERK (Extracellular Signal-Regulated Kinase) pathway. *MIAT* is further involved in SMC phenotypic transition to proinflammatory macrophage-like cells through binding to the promoter region of *KLF4* and enhancing its transcription. Studies using *Miat*^{-/-} and *Miat*^{-/-}*ApoE*^{-/-} mice, and Yucatan *LDLR*^{-/-} mini-pigs, as well, confirmed the regulatory role of this lncRNA in SMC de- and transdifferentiation and advanced atherosclerotic lesion formation.

CONCLUSIONS: The lncRNA *MIAT* is a novel regulator of cellular processes in advanced atherosclerosis that controls proliferation, apoptosis, and phenotypic transition of SMCs, and the proinflammatory properties of macrophages, as well.

Key Words: atherosclerosis ■ carotid artery diseases ■ lipoprotein(a) ■ myocytes, smooth muscle ■ RNA, long noncoding ■ stroke

Atherosclerosis is a chronic disease of intra-arterial atheromatous plaque progression that can remain asymptomatic for decades.¹ Pathologically, advanced lesions can be separated into “stable” and

“unstable” (also referred to as “vulnerable”) lesions.² Subclinical data show that plaques are most common in the iliofemoral arteries (44%), followed by the carotid arteries (31%), aorta (25%), and coronary arteries (18%).³

Correspondence to: Lars Maegdefessel, MD, PhD, Experimental Vascular Medicine Unit, Department for Vascular and Endovascular Surgery, Klinikum Rechts der Isar, Technical University Munich, Ismaninger Strasse 22, 81675 Munich, Germany. Email lars.maegdefessel@tum.de

*F. Fasolo, H. Jin, and G. Winski contributed equally.

†V. Paloschi and L. Maegdefessel contributed equally.

Supplemental Material is available with this article at <https://www.ahajournals.org/doi/suppl/10.1161/CIRCULATIONAHA.120.052023>.

For Sources of Funding and Disclosures, see page 1581.

© 2021 The Authors. *Circulation* is published on behalf of the American Heart Association, Inc., by Wolters Kluwer Health, Inc. This is an open access article under the terms of the [Creative Commons Attribution Non-Commercial-NoDerivs](https://creativecommons.org/licenses/by-nc-nd/4.0/) License, which permits use, distribution, and reproduction in any medium, provided that the original work is properly cited, the use is noncommercial, and no modifications or adaptations are made.

Circulation is available at www.ahajournals.org/journal/circ

Clinical Perspective

What Is New?

- The contribution of long noncoding RNAs to the development and progression of vascular disease remains largely unknown.
- The long noncoding RNA *Myocardial Infarction Associated Transcript (MIAT)* had previously been discovered in genome-wide association and transcriptomic profiling studies using diseased cardiovascular specimens and experimental models.
- We describe a novel role for *MIAT* in regulating proliferation and transdifferentiation of arterial smooth muscle cells and inflammatory activity in macrophages, as well, during atherosclerotic plaque development and progression.

What Are the Clinical Implications?

- Long noncoding RNAs possess key regulatory functions, directly interacting and mediating expression and functionality of proteins, other RNAs, and DNA, as well.
- The long noncoding RNA *MIAT* plays a key role during atherosclerotic plaque development and lesion destabilization. Its expression becomes highly increased in high-risk patients with vulnerable plaques.
- Therapeutic targeting of *MIAT*, using antisense oligonucleotides, offers novel treatment options for patients with advanced atherosclerosis in carotid arteries at risk of stroke.

Nonstandard Abbreviations and Acronyms

EGR1	early growth response 1
ELK1	ETS transcription factor ELK1
ERK	extracellular signal-regulated kinase
hCASMC	human carotid smooth muscle cell
KLF4	Krüppel-like factor 4
lncRNAs	long noncoding RNAs
Lp(a)	lipoprotein(a)
MIAT	Myocardial Infarction Associated Transcript
NF-κB	nuclear factor κ-light-chain-enhancer of activated B cells
oxLDL	oxidized low-density lipoprotein
SMC	smooth muscle cell

The rupture of lesions in the carotid and coronary vascular beds is the main cause of stroke and myocardial infarction, respectively. Stroke remains a massive public health problem with an increasing need for better strategies to prevent and treat the disease in our aging society.⁴ Despite surgical removal of the plaque with carotid

endarterectomy or stenting for symptomatic patients, obtaining a better understanding of the cellular mechanisms and regulatory networks driving carotid plaque development and progression is essential to identifying novel therapeutic targets.

The pathogenesis of carotid atherosclerotic lesions is orchestrated by different vascular cell subtypes.⁵ Vascular smooth muscle cell (SMC) accumulation is considered a hallmark of atherosclerosis and vascular injury.⁶ It is well documented that the aberrant proliferation of SMCs can promote plaque formation.^{6,7} Recent genetic lineage tracing studies show that SMC phenotypic switching into macrophage-like cells can promote vascular inflammation and the progression of atherosclerosis.^{8,9} In this advanced disease process, lipid loading and phagocytosis play a crucial role.^{10,11} Accumulating data suggest that constant uptake of oxidized low-density lipoprotein (oxLDL) in macrophages and SMCs can trigger foam cell formation while activating an inflammatory cascade that enhances plaque vulnerability.^{12,13}

Long noncoding RNAs (lncRNAs), defined as non-protein coding transcripts longer than 200 nucleotides, have emerged as important regulators in various biological processes and during disease development.¹⁴ However, the functional relevance during disease progression remains elusive for most of these transcripts.¹⁵ The lncRNA *Myocardial Infarction Associated Transcript (MIAT)*, also known as *Gomafu* was initially identified in a genome-wide association study in Japanese patients with myocardial infarction.¹⁶ Recent evidence suggests that *MIAT* regulates endothelial cell inflammation in diabetic retinopathies by competing as an endogenous RNA in a feedback loop with the vascular endothelial growth factor and miR-150-5p.¹⁷ Whether and how *MIAT* participates in atherosclerosis and mechanisms that destabilize advanced plaques has yet to be experimentally addressed.

We performed RNA profiling in 2 independent patient cohorts with advanced carotid plaques undergoing carotid endarterectomy. We further analyzed carotid plaques from a Yucatan *LDLR*^{-/-} mini-pig model of advanced atherosclerosis and performed mechanistic studies using vascular injury (carotid ligation) and inducible plaque rupture (ligation and cuff) in mice to establish functional relevance for *MIAT* during lesion progression and destabilization. We show that *MIAT* not only promotes proliferation of carotid SMCs through the ERK (extracellular signal-regulated kinase)-ELK1 (ETS transcription factor ELK1)-EGR1 (early growth response 1) pathway, but also regulates macrophage activation through Nuclear Factor κ-light-chain enhancer of activated B cells (NF-κB) signaling. In addition, it regulates the phenotypic transition of SMCs into macrophage-like cells through direct interaction with the promoter region of *Krüppel-like factor 4 (KLF4)* to accelerate its transcriptional activation.

METHODS

The authors declare that all data that support the findings of this study are available within the article and its [Supplemental Material](#). Detailed descriptions of materials and methods used in this study, including the preparation and transcriptomic analysis of human plaques, RNA scope in murine and human tissue, laser capture microdissection of human carotid lesions, the inducible plaque rupture model in mice, the murine carotid artery ligation model, cholesterol and triglyceride measurements in mouse plasma, in vitro cell culture and transfection, proliferation, migration, apoptosis, and oxLDL uptake assays using the kinetic live-cell imaging in murine and human cell lines, the porcine atherosclerosis model, in situ hybridization, immunohistochemical and immunofluorescent analysis, RNA immunoprecipitation, luciferase reporter assays, *MIAT* modulation in vitro and in vivo, protein extraction, and immunoblotting can be found in the [Supplemental Material](#).

Human Advanced Atherosclerotic Carotid Artery Plaques

Advanced carotid artery atherosclerotic lesions (carotid plaques) and nonatherosclerotic iliac artery controls were obtained from the Biobank of Karolinska Endarterectomies as previously published.¹⁸ RNA profiling and gene expression analysis were performed as described.¹⁸ Microarray data related to this study are available from Gene Expression Omnibus data sets (accession number GSE21545). Paraffin-embedded sections were used for in situ hybridization and immunostaining as described in the [Supplemental Material](#). Another set of independent carotid atherosclerotic plaques originate from the Munich Vascular Biobank.¹⁸ From this biobank, plaques with either a ruptured or stable plaque phenotype were analyzed and used for laser-capture microdissection experiments as described in the [Supplemental Material](#). All studies were approved by the Ethical Committee of Stockholm and Klinikum Rechts der Isar, Technical University Munich; patient informed consent was obtained according to the Declaration of Helsinki.

Statistics

Data are presented as mean±SEM, unless stated differently. Groups were compared by using the Student *t* test (2-tailed) for parametric data. Normality was tested to ensure that parametric testing was appropriate. Gene expression data were analyzed using log₂ expression values and then transformed into fold-change for presentation purposes. When comparing multiple groups, data were analyzed using ANOVA with post hoc multiple comparisons using the Tukey method. For the InCuCyte experiments, normalized data were compared by 2-way repeated-measures ANOVA (for confluence data) or area under the curve (for count data). For analysis of multiple gene expression panels, *t* tests corrected for multiple comparisons using the Holm-Sidak method were performed. Categorical data were analyzed by using the χ^2 test or Fisher exact test when 1 category was <3. A value of *P*<0.05 was considered statistically significant. All analyses were performed using GraphPad Prism version 9, except that microarray data set analyses were performed with GraphPad Prism versions 6 and 7. A linear regression model adjusted for age and sex and a 2-sided Student *t* test assuming nonequal deviation with correction for multiple

comparisons according to Bonferroni were used for analyses of the noncoding RNAs from microarrays.

RESULTS

MIAT Was Increased in Advanced Human Carotid Plaques and Important for SMC Survival

The lncRNA *MIAT* was identified as the most upregulated noncoding RNA transcript in microarray profiling comparing human carotid plaques (n=127) to nonatherosclerotic controls (n=10) from the Biobank of Karolinska Endarterectomies (Figure 1A and 1B). This result was validated by quantitative real-time polymerase chain reaction using plaques from a nonoverlapping set of patients in Biobank of Karolinska Endarterectomies (Figure S1A in the [Supplemental Material](#), 77 human carotid plaques versus 13 nonatherosclerotic controls; patient demographics are in [Table S1 in the Supplemental Material](#)).

Next, we assessed *MIAT* expression in laser-captured microdissected fibrous caps from ruptured/unstable (cap thickness ≤200 μm, n=10) compared with stable (cap thickness ≥200 μm; n=10) advanced atherosclerotic lesions from the Munich Vascular Biobank¹⁹ (Figure 1C). In these SMC-enriched fibrous caps, *MIAT* was expressed 2-fold higher (*P*=0.031) in ruptured than in stable lesions from laser-dissected tissue (Figure 1D).

RNAscope revealed coexpression of *MIAT* with SMC α -actin (α SMA)-positive cells, and to a lesser extent with CD68 (Figure 1E, [Figure S1B in the Supplemental Material](#), positive and negative controls in [Figure S2A and S2D in the Supplemental Material](#)). Conventional in situ hybridization confirmed *MIAT* being predominantly present in the medial layer of nonatherosclerotic control arteries ([Figure S3A in the Supplemental Material: ctrl_MIAT](#)). In stable plaques, *MIAT* expression was substantially elevated ([Figure S3A in the Supplemental Material, plaque_MIAT](#)) and detected predominantly in α SMA-positive cells, and to a lesser extent coexpressed with CD68 (Figure 1E, [Figures S1B and S4A in the Supplemental Material](#)).

MIAT Was Significantly Increased in Advanced Murine and Porcine Carotid Plaques and Regulated Proliferation in Vascular SMCs

To determine the mechanistic role of *MIAT* in carotid plaque development and progression, we used a murine inducible plaque rupture model using incomplete ligation and cuff placement in *ApoE*^{-/-} mice as previously described^{20,21} (Figure 2A). Consistent with the human data discussed earlier, a significant induction of *Miat* was observed in advanced murine carotid plaques compared with contralateral uninjured controls (Figure 2B). During early plaque formation using incomplete carotid

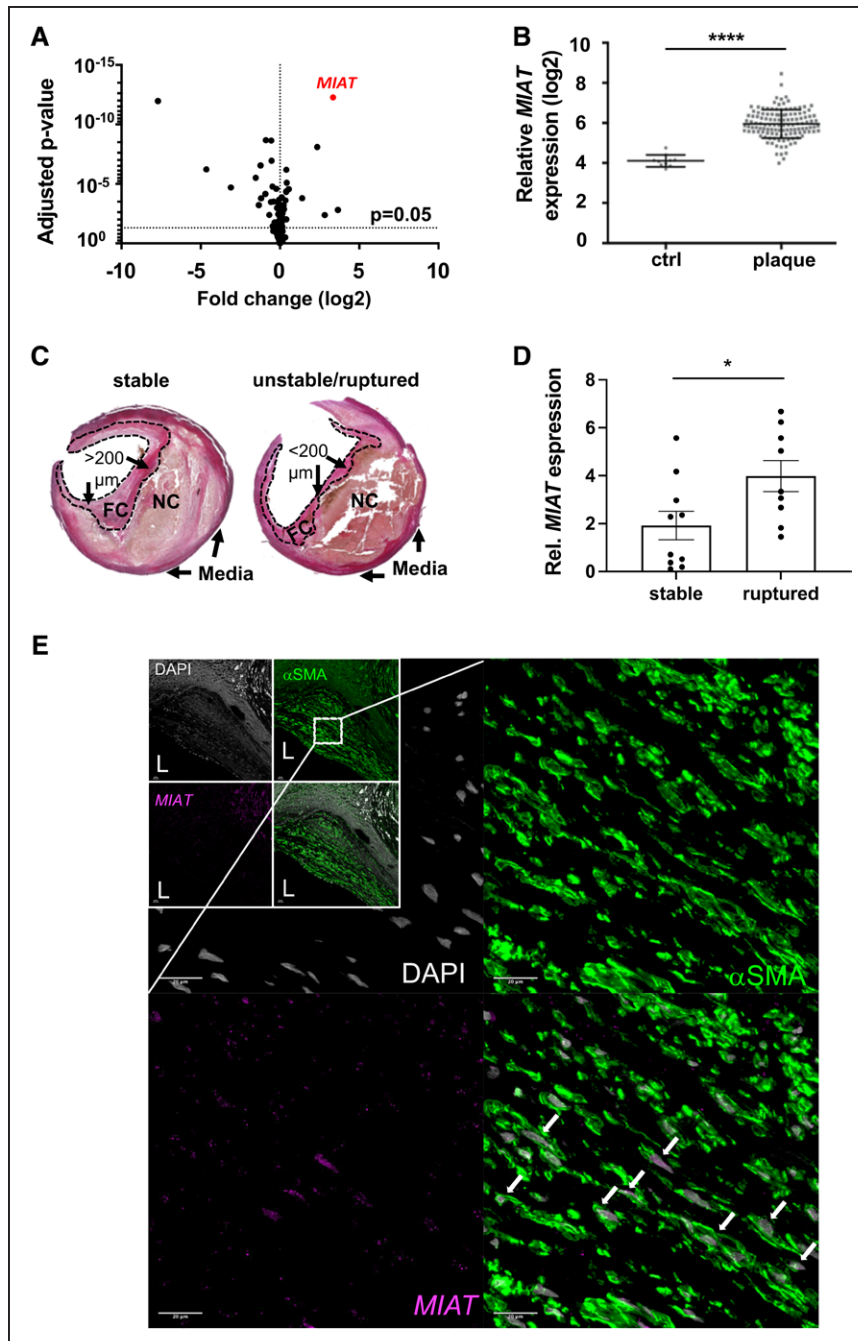


Figure 1. MIAT expression is increased in advanced stages of human carotid artery disease.

A, Scatter plot of deregulated noncoding transcripts in human carotid plaques (n=127) compared with nonatherosclerotic controls (n=10) from the Biobank of Karolinska Endarterectomies. **B**, Expression plot for *MIAT* based on the results presented in Figure 1A. **C**, Hematoxylin and eosin–stained stable and unstable/ruptured atherosclerotic lesions from the Munich Vascular Biobank. Dotted line indicates the laser-catalypted fibrous cap (FC). NC represents necrotic core. FC >200 μm was considered a stable lesion; FC <200 μm was unstable/ruptured. **D**, *MIAT* expression in laser captured microdissected stable versus ruptured fibrous caps (mean±SEM; unpaired nonparametric Student *t* test). **E**, Colocalization analysis of *MIAT* and αSMA protein was performed by RNAscope protocol. *MIAT* and αSMA protein were detected through Opal 690 and Opal 520, visualized in purple and green color, respectively. Nuclei are stained with DAPI (gray). **Upper Left**, the boxes represent overview images of the carotid plaques, and the zoomed-in images are magnifications acquired within the plaque shoulder region. White arrows highlight the nuclear detection of *MIAT* in cells expressing the smooth muscle cell marker (αSMA). Bar=100 μm. **P*<0.05; *****P*<0.0005. Data are presented as mean±SD (SEM in **D**) with Student *t* test and corrected for multiple comparison (**A**) using Bonferroni correction. Ctrl indicates control; DAPI, 4',6-diamidino-2-phenylindole; Rel., relative; and αSMA, smooth muscle cell α-actin.

ligation for 4 weeks (without cuff placement), *Miat* expression was substantially increased (Figure S4B in the Supplemental Material).

RNAscope, in situ hybridization, and immunostaining showed that *Miat* expression was induced predominantly in αSMA+ cells in the SMC-rich fibrous cap, and in the medial layer structures of progressed lesions, as well (Figure 2C, Figure S4C in the Supplemental Material). This enhanced expression pattern was associated with increased cell proliferation (Ki-67+ cells) but not apoptosis (Caspase 3+ cells; Figure S5A in the Supplemental Material, negative controls for RNAscope in Figure S5B in the Supplemental Material).

Next, we evaluated *MIAT* in advanced lesions from *LDLR*^{-/-} Yucatan mini-pigs after 6 months (early soft-plaque stage of atherosclerosis in this model) and 12 months (late and advanced atherosclerotic state) of being fed a high-fat diet (HFD; Figure 2D). Similar to the inducible plaque rupture model in mice and the expression changes in human plaques, advanced lesions (after 12 months of HFD) displayed more macrophages (indicated by the microglia/macrophage-specific ionized calcium-binding adapter molecule 1/IBA-1-positive cells) and fewer αSMA-positive cells than pigs that were on the shorter-term HFD (Figure 2E). *MIAT* expression was elevated in the more destabilized lesion phenotype (Figure 2F).

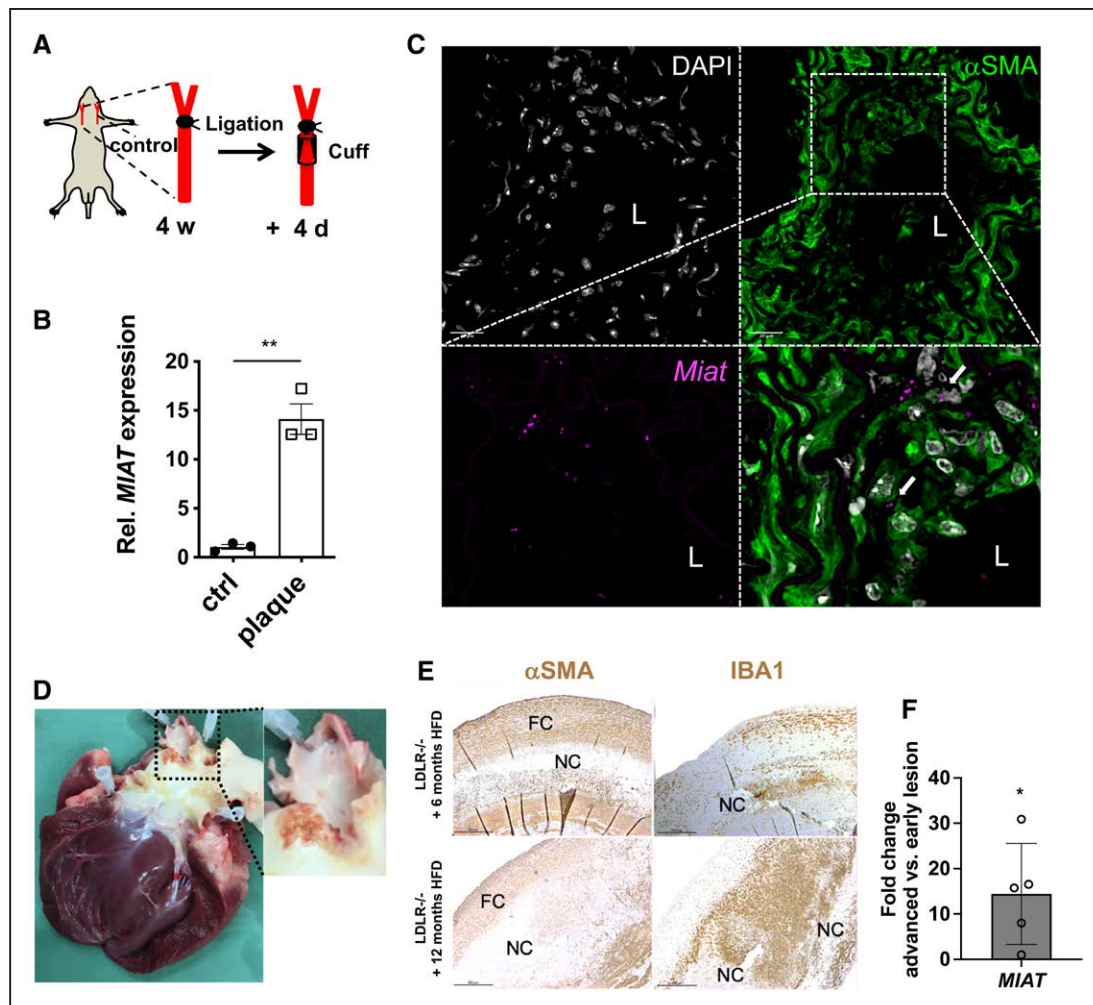


Figure 2. MIAT is significantly increased in murine carotid plaques and regulates proliferation in vascular smooth muscle cells.

A, Illustration of the inducible plaque rupture model using incomplete ligation and cuff placement in *ApoE*^{-/-} mice. **B**, Expression of *Miat* determined by quantitative real-time polymerase chain reaction from advanced plaques and contralateral controls from the inducible plaque rupture model presented in Figure 2B. **C**, Colocalization analysis of *Miat* and α SMA protein was performed by RNAscope in murine carotid plaques. *Miat* and α SMA protein were detected through Opal 690 (purple) and Opal 520 (green). Nuclei are stained with DAPI (gray). **D**, Ruptured plaque in the coronary ostia from an advanced lesion from *LDLR*^{-/-} Yucatan mini-pigs being fed 12 months of high-fat diet (HFD). **E**, Immunostaining of smooth muscle cell α -actin (α SMA) and macrophage marker-ionized calcium-binding adapter molecule 1 (IBA1) in plaques from early (6 months HFD) and advanced (12 months HFD) carotid artery lesions (FC indicates fibrous cap; NC, necrotic core). **F**, Relative *MIAT* expression in advanced (12 months HFD) versus early (6 months HFD) carotid plaques. Data were analyzed by Student *t* test. **P*<0.05; ****P*<0.001. Ctrl indicates control; DAPI, 4',6'-diamidino-2-phenylindole; L, lumen; and Rel., relative.

Modulation of *MIAT* Affected Proliferation and Apoptosis in Human Carotid Artery SMCs

To evaluate the cellular effect of *MIAT* modulation in human carotid smooth muscle cells (hCASMCs), we used a live-cell imaging system in combination with conventional immunohistochemical analysis. First, 3 different customized anti-*MIAT* GapmeRs were tested for their knockdown efficiency, and the most potent one was chosen for functional studies (Figure S5C and S5D in the Supplemental Material). Cells were dynamically monitored for rates of proliferation and apoptosis over time. Knockdown of *MIAT* (KD) limited proliferation rates and substantially enhanced apoptosis (Casp3⁺, green) of SMCs in a time- and dose-dependent manner (Figure 3A and 3B;

Figure S5E in the Supplemental Material). Immunostaining with the proliferation marker Ki-67 and apoptosis marker Caspase 3 after *MIAT* knockdown confirmed these results (Figures 3c,d).

MIAT regulated hCASMC Proliferation Through the ERK/ELK1/EGR1 Pathway

We next assessed the specific molecular mechanism through which *MIAT* mediates carotid plaque advancement and lesion destabilization. Previous data suggested that *MIAT* may act as a sponge for miR-150, which forms a negative feedback loop in the endothelium,¹⁷ cardiomyocytes,²² epithelial cells,²³ and lung cancer cells.²⁴ However, we did not detect significant changes in miR-150

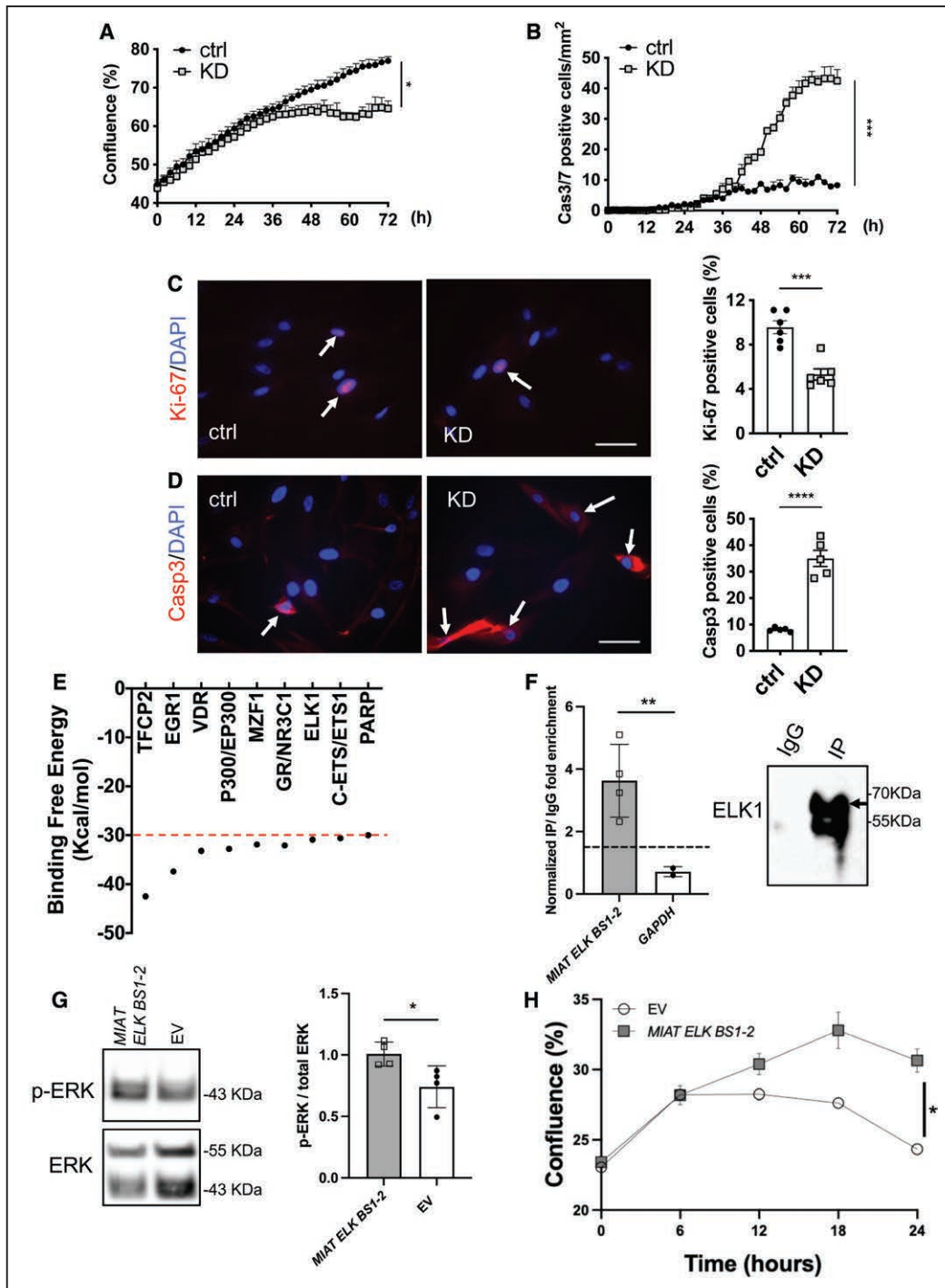


Figure 3. MIAT regulates human carotid artery smooth muscle cell proliferation through the ERK/ELK1/EGR1 pathway. **A** and **B**, Proliferation (**A**) or apoptosis (**B**) of human carotid smooth muscle cells (hCASMCs) on knockdown of *MIAT* (KD) monitored through live-cell imaging over time (0–72 hours). Data were analyzed by 2-way ANOVA. **C** and **D**, Proliferation (**C**) or apoptosis (**D**) of hCASMCs on KD of *MIAT* determined by Ki-67 or Caspase 3 immunofluorescent staining (white arrows indicate Ki-67/Caspase 3–positive cells). Bar=50 μ m. **E**, *In silico* analysis of transcription factors associated with *MIAT* (predicted binding free energy of -30 Kcal/mol) using the regulatory RNA elements/RegRNA tool. **F**, *MIAT* fragment containing 2 predicted ELK1 binding sites (*MIAT*-ELK1_BS1_BS2) was transiently transfected and coimmunoprecipitated with endogenous ELK1 in hCASMCs. IgGs were used as control of immunoprecipitation (IP) specificity. *MIAT* or *GAPDH* (as unrelated target) enrichment in ELK1 IP fraction was quantified with quantitative real-time polymerase chain reaction and expressed as $(2^{\Delta\Delta Ct}) \times 100$ ELK1 IP \div $(2^{\Delta\Delta Ct}) \times 100$ IgG. $\Delta\Delta Ct$ was calculated based on input. RNA content in IP or IgG was normalized on RPLP0 mRNA. ELK1 IP efficiency was monitored by Western blot using an anti-ELK1 antibody. **G**, Transfected cells were lysed after 24 hours, and total protein was extracted. P-ERK normalized to total ERK was monitored using Western Blot. Quantification of the Western Blot was done with Fiji Image J software. **H**, *MIAT*-ELK1_BS1_BS2 was transiently transfected, and proliferation was monitored using the IncuCyte Live Cell Imaging System. Bar=50 μ m. Data were analyzed by 2-way repeated-measures ANOVA (**A**), area under the curve (**B**), and Student *t* test (**C**, **D**, **F**, **G**). * $P<0.05$; ** $P<0.01$; *** $P<0.001$; **** $P<0.0001$. Casp indicates caspase; Ctrl, control; DAPI, 4',6-diamidino-2-phenylindole; EV, empty vector (control); and IgG, immunoglobulin G.

in human carotid plaques or cultured hCASCs after *MIAT* modulation (Figure S6A and S6B in the Supplemental Material), suggesting that the influence of *MIAT* on SMCs in advanced atherosclerosis is not mediated through its miR-150 interaction.

Transcription factors are master regulators controlling gene expression, chromatin stability, and cell homeostasis.^{25–27} To explore how *MIAT* regulates SMC proliferation, we hypothesized that it might affect molecular processes through alteration of transcription factors. On the basis of an *in silico* analysis using the regulatory RNA elements/*RegRNA* tool,²⁸ we identified several transcription factors that potentially interact with *MIAT* but still require experimental validation: transcription factor CP2 (*TFCP2*), early growth response 1 (*EGR1*), vitamin D receptor (*VDR*), E1A binding protein 300 (*P300/EP300*), myeloid zinc finger 1 (*MZF1*), nuclear receptor subfamily 3 group C member 1 (*GR/NR3C1*), ETS transcription factor (*ELK1*), ETS proto-oncogene 1 (*C-ETS/ETS1*), and poly (AD-Ribose) polymerase (*PARP*). According to *RegRNA*, these transcription factors have a predicted binding free energy of < -30 kcal/mol (Figure 3E). To determine whether these transcription factors are regulated by *MIAT*, a custom-designed mRNA array investigating changes in expression for these transcription factors in SMCs after knockdown of *MIAT* was performed as previously described.²⁹

Results revealed that *EGR1*, *ELK1*, and *GR/NR3C1* were downregulated after knockdown of *MIAT* (Figure S6C in the Supplemental Material). *EGR1* deficiency is associated with reduced plaque development in hyperlipidemic mice highlighting its importance in human atherosclerosis.³⁰ Increased ERK signaling and p-ELK1/ELK1 binding to the proximal *EGR1* promoter region influence *EGR1* transcription.^{31,32} Because both components of this pathway, *EGR1* and *ELK1*, were downregulated by *MIAT* inhibition, we investigated a potential direct interaction. Inhibition of *MIAT* limited phosphorylation of ERK (p-ERK), augmented accumulation of p-ELK1 in the nucleus, and subsequently reduced *EGR1* expression, which overall accounted for a loss in SMC proliferation (Figure S6D and S6E in the Supplemental Material). Similar results could be observed in PDGF-BB (platelet-derived growth factor BB) prestimulated SMCs (Figure S7A in the Supplemental Material). Isolation of the nuclear and cytoplasmic fraction of hCASCs followed by quantitative real-time polymerase chain reaction revealed a predominant nuclear expression of *MIAT* (Figure S7B in the Supplemental Material), leading to the hypothesis of a possible direct interaction of the lncRNA with transcriptionally active complexes. To investigate the contribution of *MIAT* to ERK signaling, we assessed its binding with *ELK1* through RNA immunoprecipitation. Enrichment of *MIAT* in the *ELK1*-immunoprecipitated fraction (Figure 3F) supports the hypothesis of a *MIAT*-mediated transcriptional regulation at the *EGR1* locus. In line with this, *MIAT* over-

expression increased ERK phosphorylation (Figure 3G) and augmented hCASCs proliferation (Figure 3H).

Moreover, increased *MIAT* levels correlated positively with *EGR1* expression in proliferative SMCs (α SMA and Ki-67+) in human carotid plaques (Figure S7C in the Supplemental Material). The upregulation of *EGR1* and *ELK1* were also confirmed using quantitative real-time polymerase chain reaction in human and mouse carotid plaques (Figure S7D and S7E in the Supplemental Material).

MIAT Was Increased in Patients With Elevated Circulating Lipoprotein(a) Levels

To further dissect the role of *MIAT* in atherosclerosis, we examined its expression in advanced human carotid plaques in relation to various clinical parameters of patients with carotid artery disease (plasma lipid profile, C-reactive protein, body mass index, hemoglobin A1c, creatinine, medications, etc; see Table S2 in the Supplemental Material). We discovered that *MIAT* expression in plaques was substantially elevated and correlated with higher plasma levels of lipoprotein(a) (Lp[a]), an important risk factor and potential novel therapeutic target in cardiovascular disease^{33–35} (Figure 4A). No significant correlation was observed for *MIAT* and other determinants of plasma lipid levels (triglycerides, low-density lipoproteins, and high-density lipoproteins; Table S2 in the Supplemental Material). We further assessed this finding *in vitro*, where treatment with lipoprotein(a) (Lp[a]) significantly increased *MIAT* in a dose-dependent manner (Figure 4B) and induced proliferation and limited apoptosis of SMCs. The knockdown of *MIAT* attenuated these effects in SMCs (Figure 4C and 4D), indicating that *MIAT* crucially regulates SMC dynamics and thus fibrous cap stability when elevated Lp(a) levels are present in atherosclerotic plaques.

Last, we used 2 apo(a) peptide constructs with and without an attached oxidized phospholipid³⁴ (17K and 17KDelta, respectively; Figure 4E) to determine their specific importance for Lp(a)-dependent stimulation of *MIAT* and subsequent regulation of SMCs. The wildtype 17K containing oxidized phospholipid (17K) significantly stimulated *MIAT* production (Figure 4E) and enhanced SMC proliferation. This effect was not observed using the 17KDelta variant (Figure 4F) lacking oxidized phospholipids. Previous findings have determined that downstream Lp(a) effects appear largely executed by the oxidation of phospholipids.³⁶ Here, we investigated the effect of blocking oxidized phospholipids on Lp(a) by treating SMCs with a novel humanized mouse antibody targeting the oxidized phosphocholine head of phospholipids ATH3G10.³⁷ ATH3G10 blocked *MIAT* expression in Lp(a)-prestimated SMCs (Figure S8A in the Supplemental Material), thereby confirming the key role oxidized phospholipids play in Lp(a)-mediated vascular disease exacerbation.

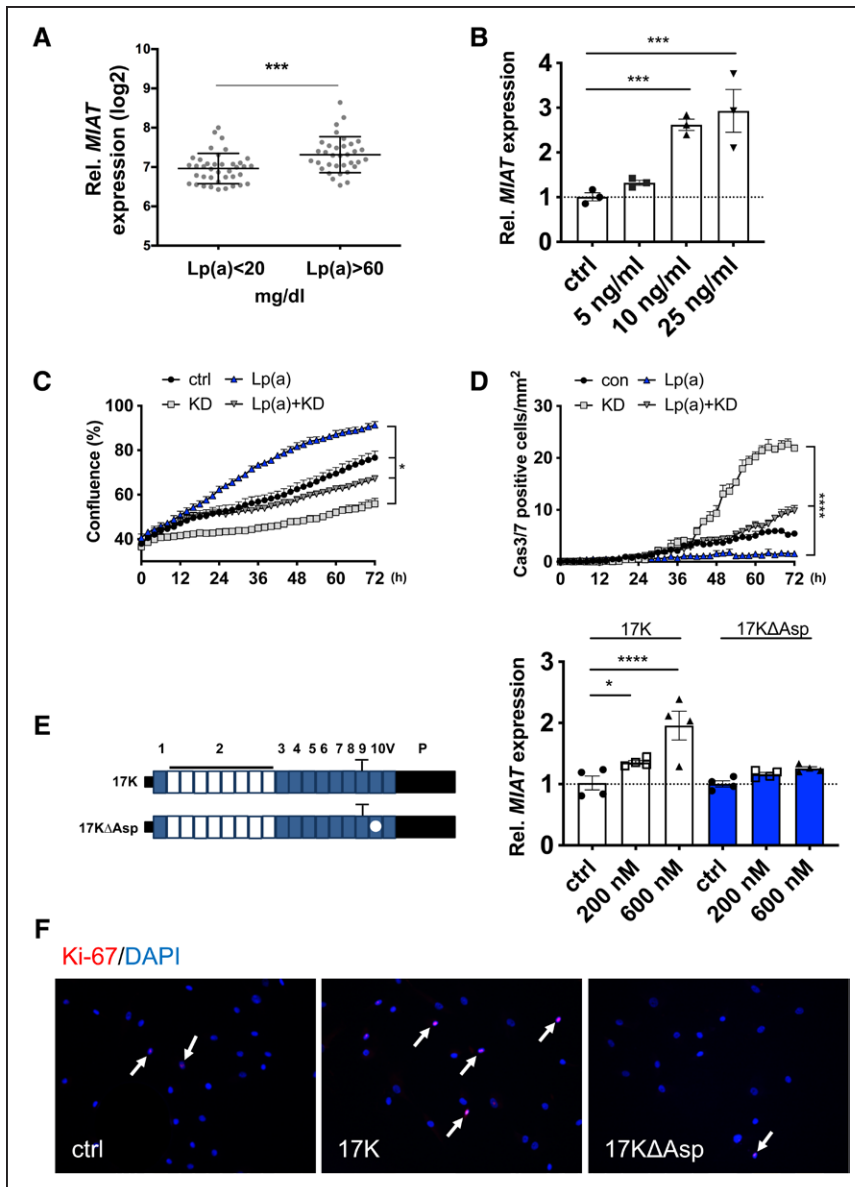


Figure 4. MIAT is increased in patients with elevated circulating lipoprotein(a) levels.

A, Expression of *MIAT* in patients in Biobank of Karolinska Endarterectomies with low (<20 mg/dL) and high (>60 mg/dL) lipoprotein(a) (Lp[a]) serum levels. **B**, Expression of *MIAT* in hCASCs on Lp(a) stimulation. **C** and **D**, Proliferation (**C**) or apoptosis (**D**) of hCASCs on *MIAT* knockdown (KD), Lp(a) or combined treatment monitored live-cell imaging over time (data were analyzed by 2-way ANOVA). **E, Left**, Schematic of APO(a) peptide constructs with (17K) or without (17KΔAsp) an attached oxidized phospholipid. **E, Right**, Expression of *MIAT* in hCASCs on 17K or 17KΔAsp stimulation. **F**, Immunostaining of Ki-67 in hCASCs with 17K or 17KΔAsp stimulation (white arrows indicate Ki-67-positive cells). Data were analyzed by Student *t* test (**A**), 2-way repeated-measures ANOVA (**C**), area under the curve (**D**), or 1-way ANOVA (**B, E**). **P*<0.05; ****P*<0.001; *****P*<0.0001. Cas indicates caspase; ctrl, control; DAPI, 4',6'-diamidino-2-phenylindole; and Rel., relative.

MIAT Triggered Inflammation and Macrophage Activity in Advanced Atherosclerotic Lesions

Inflammation, matrix degradation, and macrophage activity play a decisive role in atherosclerotic lesion formation.^{10,11,35} A significant positive correlation between *MIAT* and inflammatory and matrix degradation indicators, such as transforming growth factor β 1 (*TGF β 1*) and matrix metalloproteinase-2 (*MMP2*) was detected in advanced lesions (Figure S8B and S8C in the Supplemental Material).

The plaque microarray data consistently revealed that *MIAT* was not only significantly correlated with SMC marker genes such as actin alpha 2 (*ACTA2*), smoothelin (*SMTN*), and myosin heavy chain 11 (*MYH11*), but also several indicators of macrophage activity (such as *CD80*, *CD36*, *CD163*, *CD40*), cell proliferation (*PCNA* and *NF- κ B1*), and inflammatory cytokines and growth factors

including interleukins 6, 10 and 1 β (*IL6*, *IL10*, and *IL1 β*), *TGF β 1*, platelet-derived growth factor β (*PDGF β*), and tumor necrosis factor α , as well (*TNF α* ; Table S3 in the Supplemental Material).

To confirm that *MIAT* contributes to macrophage activity and is of relevance to inflammation in advanced lesions, we first evaluated their ability to internalize oxLDL and transform into foam cells. The knockdown of *MIAT* caused a reduction in oxLDL uptake in human monocyte-derived macrophages (Figure 5A and 5B). In addition, *MIAT* was markedly elevated in THP1-derived macrophages, which exerted a proinflammatory phenotype following lipopolysaccharide stimulation (Figure 5C, Figure S8D in the Supplemental Material). In contrast, lower expression rates of *MIAT* were seen in conjunction with IL4 (interleukin 4) pretreatment (Figure 5D, Figure S8E in the Supplemental Material), linking *MIAT* to a more proinflammatory macrophage phenotype in ath-

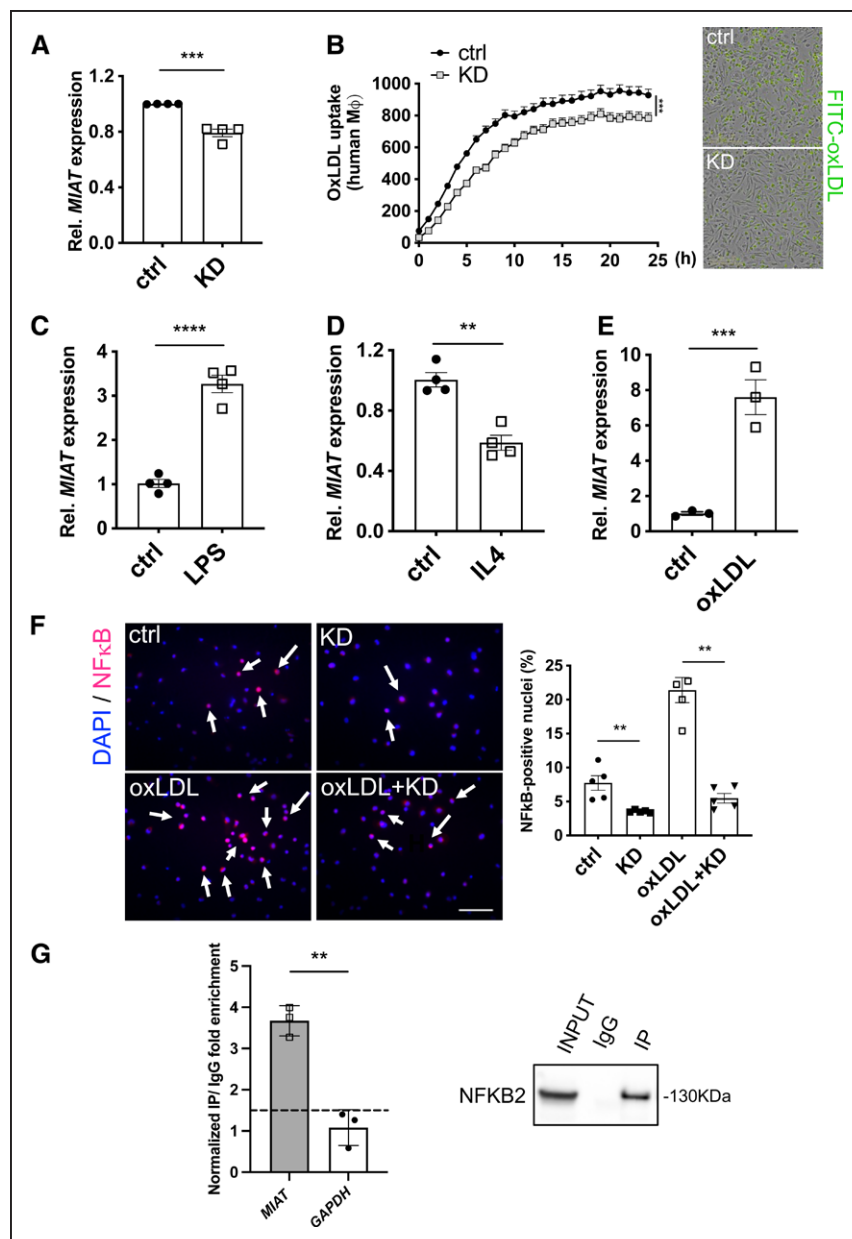


Figure 5. MIAT triggers inflammation and macrophage activity in advanced atherosclerotic lesions.

A, Expression of *MIAT* in human monocyte-derived macrophages on *MIAT* knockdown (KD). **B**, Uptake of fluorescence-labeled oxLDL in human monocyte-derived macrophages on *MIAT* KD monitored through live-cell imaging and analyzed by 1-way ANOVA. **C**, Expression of *MIAT* in human monocyte-derived macrophages on stimulation with oxLDL. **D** and **E**, Expression of *MIAT* in THP1-derived macrophages stimulated with LPS (**D**) or IL4 (**E**). **F**, Immunostaining of NF- κ B in human monocyte-derived macrophages on oxLDL stimulation with or without *MIAT* KD. Quantification is shown on the right side. **G**, Binding of endogenous *MIAT* to NF κ B2/p52/p100 in THP1 cells. *MIAT* expression in THP1 cells was triggered by oxLDL stimulation and immunoprecipitation with NF κ B2/p52/p100 or control IgG performed. *MIAT* or *GAPDH* (as unrelated target) enrichment in NF κ B2 IP fraction were quantified with real-time quantitative polymerase chain reaction. Data were analyzed by Student *t* test (**A**, **C**–**E**, **G**), AUC (**B**), or Mann-Whitney *U* test (**F**). Bar=50 μ m. ** P <0.01; *** P <0.001; **** P <0.0001. ctrl indicates control; DAPI, 4',6-diamidino-2-phenylindole; FITC, fluorescein isothiocyanate; IgG, immunoglobulin G; IL4, interleukin 4; IP, immunoprecipitation; LPS, lipopolysaccharide; NF- κ B, Nuclear Factor κ -light-chain enhancer of activated B cells; oxLDL, oxidized low-density lipoprotein; and Rel., relative.

erosclerosis. Lipid loading using oxLDL also significantly increased *MIAT* expression levels (Figure 5E).

Next, we explored how *MIAT* affects molecular processes and inflammatory signaling in macrophages. We discovered that under nonstimulated (control) conditions, NF- κ B activity remained at relatively low levels (Figure 5F). When challenged with oxLDL, NF- κ B became activated, as indicated by its translocation into the nuclei of macrophages. This nuclear translocation was completely attenuated by *MIAT* knockdown (Figure 5F). OxLDL uptake was consistently substantially impaired after treatment with an NF- κ B translocation inhibitor (Figure S8F in the Supplemental Material). *MIAT* knockdown further limited expression of transporters involved in cellular oxLDL uptake (*CD36*; steroid receptor RNA activator, *SRA*), whereas mediators

of cholesterol efflux (ATP Binding Cassette Subfamily Members: *ABCA1* and *ABCG1*) remained unchanged (Figure S8G and S8H in the Supplemental Material). These data suggest that *MIAT* facilitates NF- κ B activation and translocation during plaque progression and destabilization. Similar changes in NF- κ B activation and translocation were present in peritoneal mouse macrophages (Figure S9A and S9B in the Supplemental Material). A direct *MIAT*-NF- κ B interaction (with NF κ B2/p52/p100) was confirmed by RNA immunoprecipitation in THP1 cells (Figure 5G), where *MIAT* expression was induced through oxLDL stimulation. The NF- κ B interaction with NF- κ B-interacting lncRNA (*NKILA*)³⁸ served as a positive control for the RNA immunoprecipitation experiment (Figure S8G in the Supplemental Material).

MIAT Participated in SMC Transdifferentiation Into Inflammatory Macrophage-Like Cells Through KLF4

SMC phenotypic switching plays a key role during the development and progression of atherosclerotic lesions.^{8,39} OxLDL stimulation induced the SMC phenotypic transition to inflammatory macrophage-like cells, evidenced by downregulation of SMC markers (ACTA2, Transgelin, Myosin heavy chain 11) and elevation of phagocytosis and macrophage markers (CD68, Galectin 3; Figure 6A). This shift in cellular content and marker gene expression was also evident in stable versus ruptured human carotid arteries (Figure S9C and S9D in the Supplemental Material). MIAT inhibition in oxLDL-primed SMCs did alter expression of the cholesterol sensing gene low density lipoprotein receptor (*LDLR*), but not of 3-hydroxy-3-methylglutaryl-coenzyme A reductase (*HMGCR*; Figure S9E in the Supplemental Material).

The proinflammatory transdifferentiation process could be blocked in vitro by inhibiting MIAT expression (Figure 6A). Recent studies identified Krüppel-like factor 4 (KLF4) as a key transcription factor mediating the SMC-macrophage transition.^{8,9} We observed a remarkable induction of KLF4 after oxLDL stimulation in hCASCs (Figure 6B and 6D), and in advanced human (Figure S9F in the Supplemental Material) and mouse carotid plaques (Figure S9G in the Supplemental Material). The coeffectors ELK1 and HDAC2 were also increased (Figure 6B). The knockdown of MIAT successfully reversed these changes and decreased *KLF4*, *ELK1*, and *HDAC2* expression (Figure 6B). MIAT knockdown was further able to limit KLF4 on Lp(a) stimulation (Figure S10A in the Supplemental Material). Thus, MIAT participates in oxLDL/Lp(a)-induced SMC-macrophage transition through inducing *KLF4* expression.

To thoroughly dissect the molecular mechanism of how MIAT interacts with KLF4, we used the lncRNA:DNA interaction prediction tool *LongTarget*,⁴⁰ which predicted a putative MIAT-KLF4 promoter-binding pattern for human and mouse (Figure 6D). To assess the transcriptional activity, we conducted a luciferase reporter assay using the *KLF4/Klf4* promoter region. Human CASCs were transfected with the pLS-KLF4 promoter luciferase vector, with or without oxLDL stimulation. OxLDL stimulation led to an induction of luciferase activity, representing the transcriptional activity of *KLF4*, here serving as a positive control (Figure 6E). Knockdown of MIAT (MIAT KD) was able to block the oxLDL-induced transcription of *KLF4* completely. In contrast, overexpression of *Miat* enhanced the transcriptional activity of the *Klf4* promoter (*Klf4* promoter_ *Miat*) in mouse aortic SMCs (Figure 6F) compared with control (promoter-flanking region) without predicted *Miat* binding sites. In summary, these experiments suggest that MIAT acts as an enhancer of *KLF4* transcription through direct interaction with its promoter.

Miat Deletion Affected SMC Proliferation and Plaque Vulnerability in Vivo

For in vivo investigations into *Miat*-mediated SMC proliferation, *Miat*^{-/-} mice and their respective wildtype controls were exposed to carotid ligation, enabling us to investigate their responsiveness to stenotic flow obstruction. *Miat*^{-/-} mice presented with substantially less proliferation and increased apoptosis in their SMC-enriched intima-medial layers. α SMA-positive cells were significantly decreased in *Miat*^{-/-} mice after vascular injury (Figure 7A and 7B). SMCs derived from *Miat*^{-/-} mice also displayed a decreased migratory capacity and a higher rate of apoptosis compared with *Miat*^{+/+} controls when assessed with live-cell imaging over time (Figure S10B and S10C in the Supplemental Material). Overall, *Miat*-depleted murine SMCs displayed changes similar to human carotid SMCs after MIAT knockdown.

To further assess the role of MIAT in plaque destabilization, we cross-bred *Miat*^{-/-} with *ApoE*^{-/-} mice and exposed them to the inducible plaque rupture model. Here, *Miat*^{-/-} *ApoE*^{-/-} mice presented with thinner fibrous caps and a more unstable plaque phenotype when assessing plaque rupture rates (Figure 7C and 7G). The direct *Miat* targets *Egr1* and *Elk1* were substantially repressed in advanced lesions of *Miat*^{-/-} *ApoE*^{-/-} mice compared with littermate *Miat*^{+/+} *ApoE*^{-/-} control mice (Figure S10D in the Supplemental Material), which explains the less proliferative SMC phenotype in response to ligation and cuff placement. Atherogenesis and overall plaque development were however significantly augmented in *Miat*^{-/-} *ApoE*^{-/-} mice compared with their *Miat*^{+/+} *ApoE*^{-/-} littermate controls (Figure 7F), which we attribute to reduced expression levels of *Klf4* in double-knockout mice (Figure S10D in the Supplemental Material). Lack of *Klf4* in SMCs has previously been shown to augment the development of atherosclerosis.⁹ Lipid levels and lipid profile (total cholesterol, low density lipoprotein, very low-density lipoprotein, high density lipoprotein, triglycerides) were not altered between *Miat*^{-/-} *ApoE*^{-/-} and *ApoE*^{-/-} mice (Figure S10E in the Supplemental Material). This strongly suggests that limited plaque development in the double-knockout mice is a distinct process that initiates within the vascular wall.

Similar to the murine data described earlier, we were able to detect higher expression levels of MIAT, *KLF4*, *EGR1*, and *ELK1* (Figure S10F in the Supplemental Material) in Yucatan *LDLR*-deficient mini-pigs with more severe lesions (12 versus 6 months HFD).

DISCUSSION

Increasing evidence for lncRNAs suggests that they are involved in numerous important biological events, such as serving as scaffolding proteins, shaping nuclear architecture, imprinting genomic loci, and regulating transcriptional activity.⁴¹ The aberrant expression or mutation

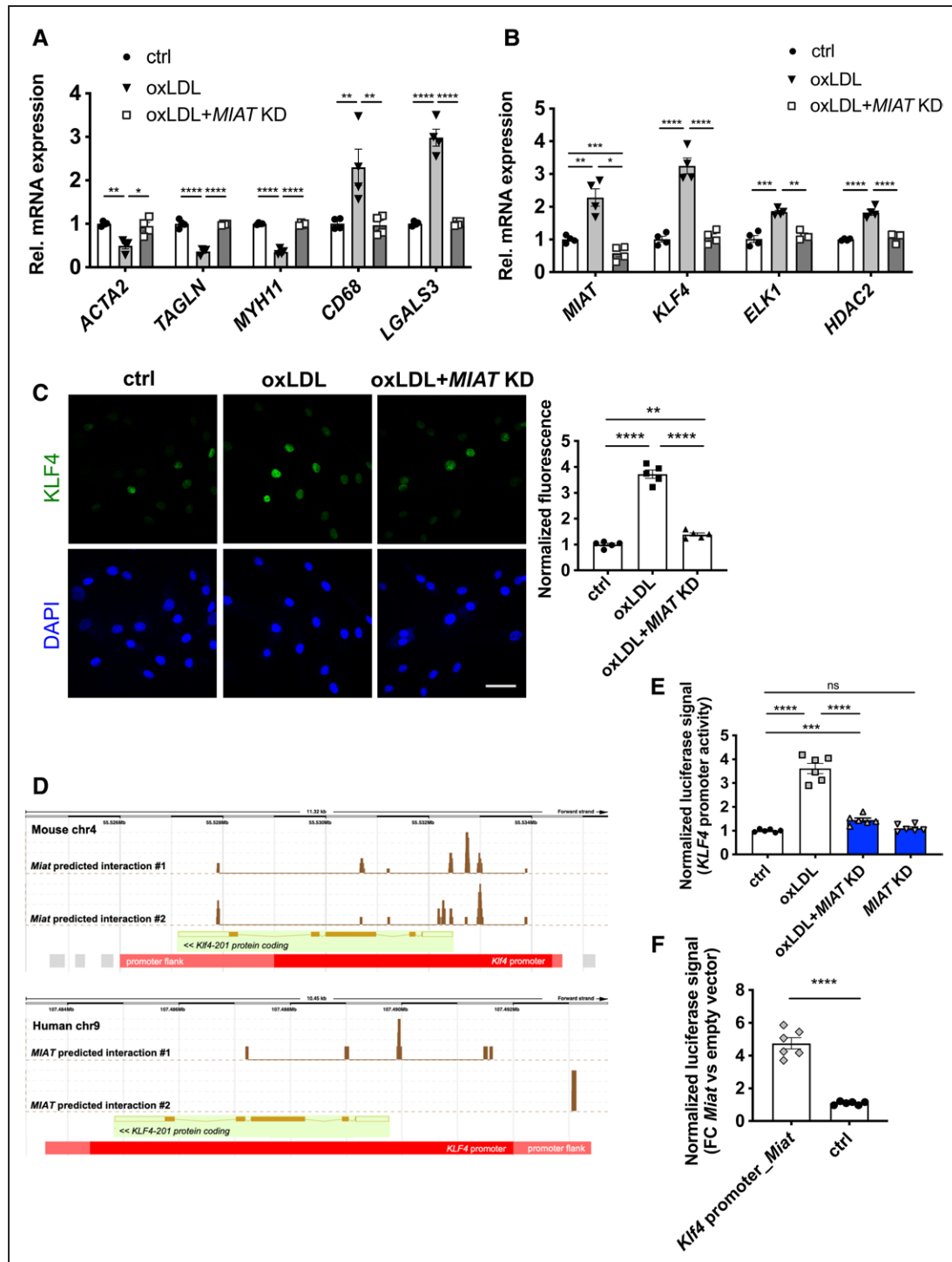


Figure 6. MIAT participates in smooth muscle cell transdifferentiation into inflammatory macrophage-like cells through KLF4 activation.

A, Expression of SMCs, phagocytosis and/or macrophage markers in hCASCs stimulated with oxLDL and with or without MIAT knockdown (KD). **B**, Expression of MIAT, transcription factor KLF4, cofactors ELK1 and HDAC2 in hCASCs stimulated with oxLDL and with or without MIAT KD. **C, Left**, Immunostaining of KLF4 in hCASCs stimulated with oxLDL and with or without MIAT KD; **Right**, fluorescence quantification. **D**, Interaction of *Miat*/MIAT with *Klf4*/*KLF4* promoter as predicted by *LongTarget v2.1*. Peaks indicate predicted binding sites of *Miat*/MIAT within *Klf4*/*KLF4* promoter region. **E**, Luciferase reporter assay with human *KLF4* promoter on oxLDL stimulation/MIAT KD in hCASCs. **F**, Luciferase reporter assay with murine *Klf4* promoter (containing *Miat* predicted binding sites; *Klf4* promoter_Miata) or promoter flanking regions (harboring no predicted *Miat* binding sites; Ctrl) in mouse aortic SMCs on *Miat* overexpression (*pCAG-Miat*, murine). Bar=50 μ m. Data were analyzed by 1-way ANOVA: * $P < 0.05$; ** $P < 0.01$; *** $P < 0.001$; **** $P < 0.0001$; P value > 0.05 indicates no significance. ctrl indicates control; DAPI, 4',6-diamidino-2-phenylindole; FC, fibrous cap; hCASC, human carotid smooth muscle cell; KLF4, Krüppel-like factor 4; oxLDL, oxidized low-density lipoprotein; Rel., relative; and SMC, smooth muscle cell.

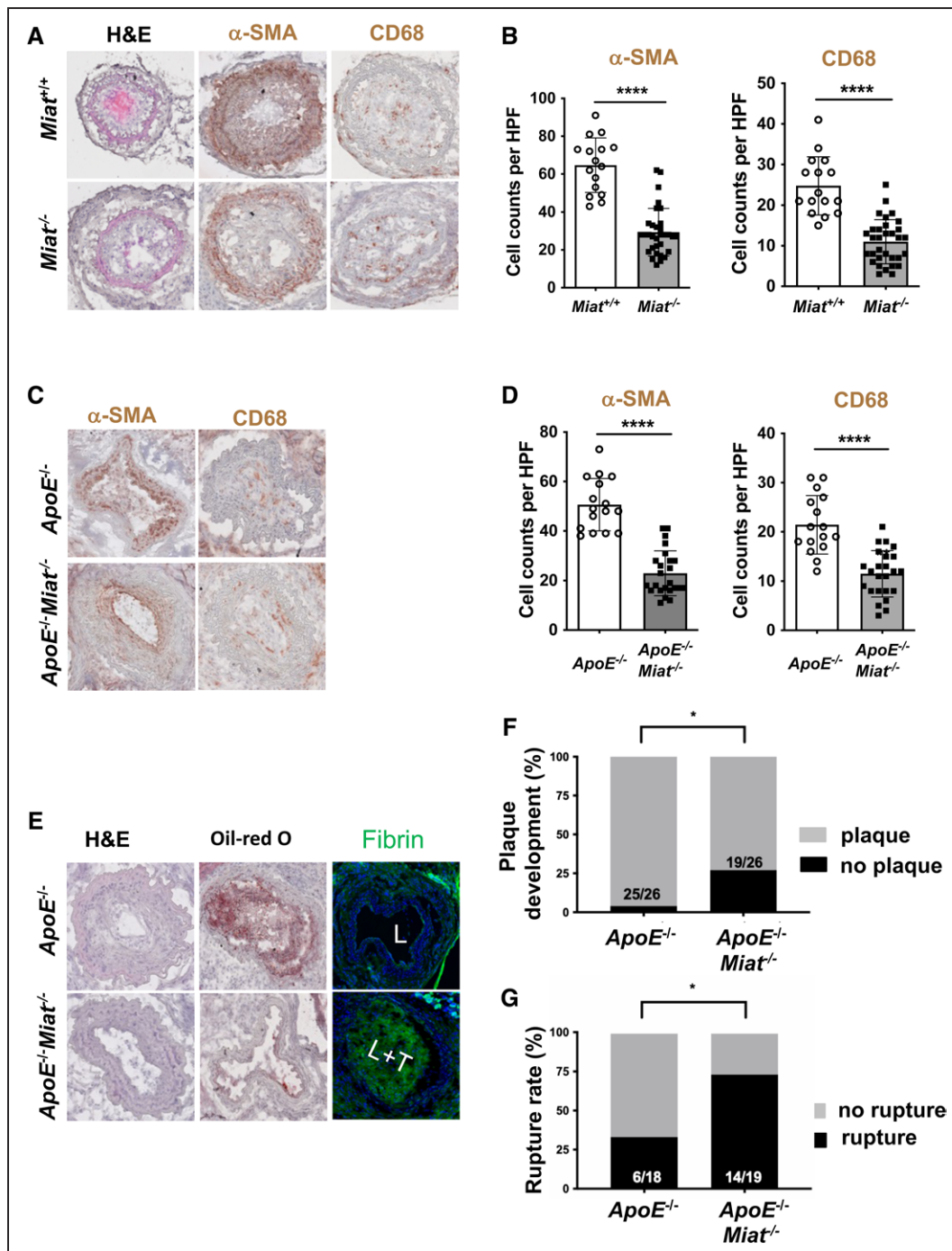


Figure 7. MIAT deletion affects smooth muscle cell proliferation and plaque vulnerability in vivo.

A, Morphology (H&E), immunostaining for CD68 and smooth muscle cell α -actin (α SMA) in *Miat*^{-/-} mice versus littermate *Miat* wildtype controls on carotid ligation injury. **B**, Analysis of cell counts (8 times/animal) per high-power field (HPF) for α SMA and CD68 from **A**. **C**, Morphology (H&E), immunostaining for CD68 and α SMA in *ApoE*^{-/-}*Miat*^{-/-} and *ApoE*^{-/-} (*Miat* wildtype) controls on exposure to the inducible plaque rupture model (incomplete ligation and cuff placement). **D**, Cell counts (8 times/animal) per HPF for α SMA and CD68 from **C**. **E**, H&E, Oil-Red O (indicating lipid deposition), and cross-linked immunofluorescent fibrin staining (indicating an atherothrombotic event) in *ApoE*^{-/-}*Miat*^{-/-} versus *ApoE*^{-/-} *Miat*^{+/+} littermate controls (L indicates lumen; L+T, lumen with thrombus). **F**, Plaque development (in %) when using the inducible plaque rupture model in *ApoE*^{-/-}*Miat*^{-/-} versus *ApoE*^{-/-}*Miat*^{+/+} mice. **G**, Rupture ratio (in %) in the inducible plaque rupture model comparing *ApoE*^{-/-}*Miat*^{-/-} versus *ApoE*^{-/-} (*Miat* wildtype) controls. Data were analyzed by Student *t* test (**B**, **D**). Fisher exact test was used to determine plaque development and rupture ratio. **P*<0.05; ***P*<0.01. H&E indicates hematoxylin and eosin.

of lncRNA genes has been implicated in various human diseases.¹⁴ In particular, in vascular biology and disease, several lncRNAs have been reported as important func-

tional regulators of endothelial cells and SMCs, such as *lincRNA-p21*,⁴² *ANRIL*,^{43,44} *SENCR*,^{45,46} *MALAT1*,⁴⁷ *SNHG12*,⁴⁸ *Tie-1AS*,^{49,50} and *CARMN*.⁵¹ In our present

study, we identified a novel molecular mechanism through which the lncRNA *MIAT* controls proliferation, apoptosis, and phenotypic transition of SMCs, and drives proinflammatory macrophage activity during foam cell and necrotic core formation, as well.

MIAT, also known as *RNCR2* (retinal noncoding RNA 2) and *Gomafu*,^{52,53} shows extensive evolutionary and functional conservation among mammals. It was first identified as a novel transcript that confers a genetic risk of myocardial infarction in a Japanese cohort.¹⁶ Later, it was shown to associate with cardiac hypertrophy,²² diabetic cardiomyopathy,⁵⁴ and cardiac fibrosis,⁵⁵ mainly by acting as a sponge for different miRNAs. In addition, *MIAT* regulates diabetes-induced microvascular dysfunction by competing with endogenous vascular endothelial growth factor and miR-150 in retinal endothelial cells. Qin et al⁵⁶ also confirmed that *Miat* promotes neurovascular remodeling in the eye and brain. *Miat* knock-down leads to cerebral microvascular degeneration, progressive neuronal loss and neurodegeneration, and behavioral deficits in Alzheimer disease, as well.⁵⁶ Our current data suggest that *MIAT* may not only play a cru-

cial role in microvascular diseases, but also macrovascular diseases such as carotid stenosis and ischemic forms of stroke (Figure 8D).

We discovered an upregulation of *MIAT* in human and murine advanced carotid plaques, where it was coexpressed and relevant for both, lesional SMCs and macrophages. The aberrant proliferation of SMCs is considered a hallmark of carotid plaque formation and progression.^{6,7} SMCs with high *MIAT* expression displayed a more proliferative status in our murine vulnerable plaque rupture model, and in human advanced lesions, as well, than those with low expression. Furthermore, increased *MIAT* expression levels or Lp(a) treatment significantly promoted proliferation of in vitro cultured hCASCs, whereas the loss of *MIAT* manifested the opposite phenotype. Increased Lp(a) levels are closely linked to atherosclerosis development and progression.^{32,57} Indeed, our data from advanced human carotid lesions indicate a positive correlation for high Lp(a) levels and *MIAT* expression. Inhibition of *MIAT* strongly mediated the consequences of Lp(a) stimulation in SMCs.

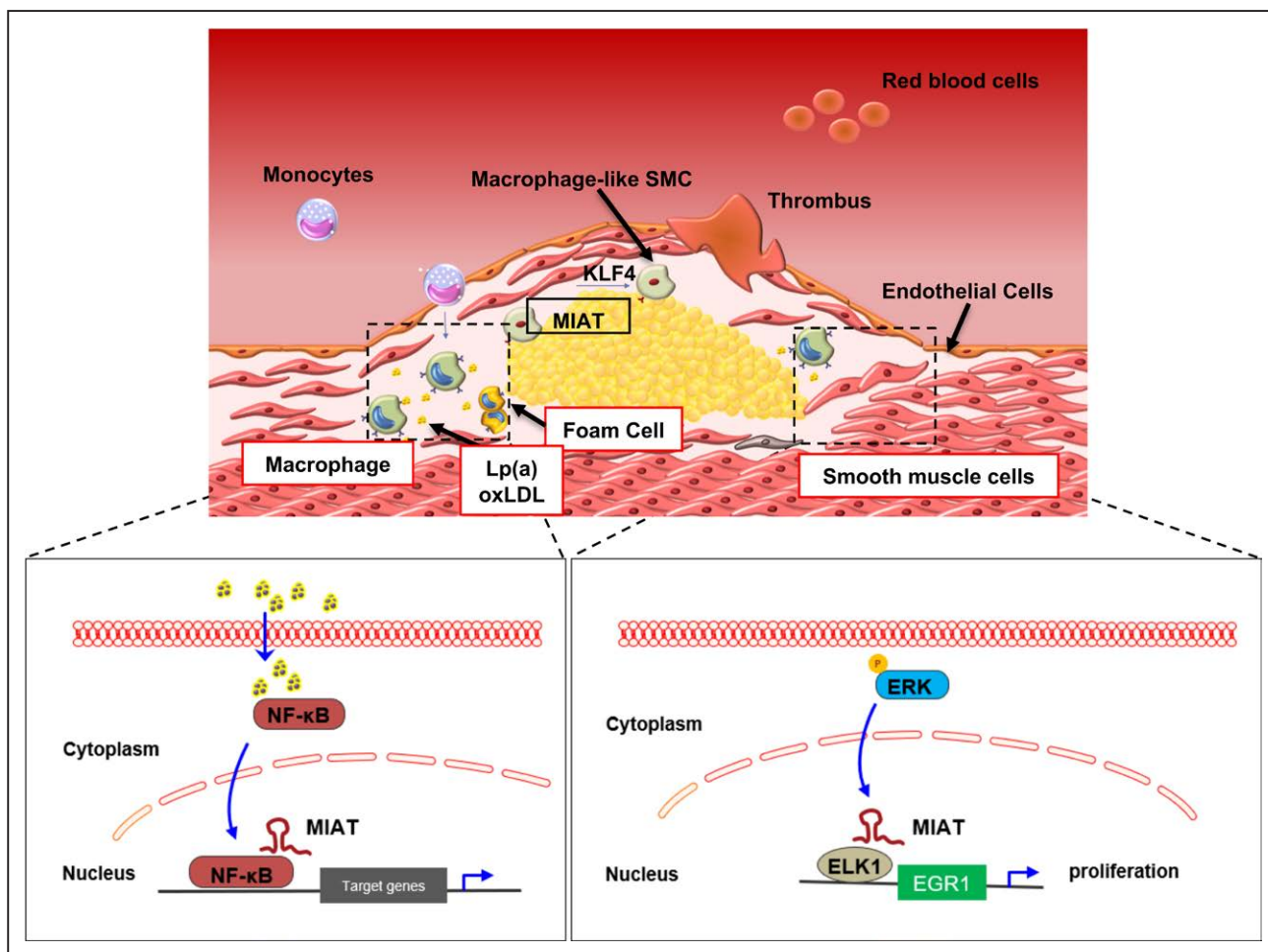


Figure 8. Proposed mechanism of action for *MIAT* in advanced atherosclerosis and plaque destabilization.

KLF4 indicates Krüppel-like factor 4; Lp(a), lipoprotein(a); NF-κB, Nuclear Factor κ-light-chain enhancer of activated B cells; oxLDL, oxidized low-density lipoprotein; and SMC, smooth muscle cell.

EGR1 is an inducible protein that belongs to the early growth response gene family and has been implicated in cellular proliferation, differentiation, and engagement with cell death pathways in vascular cells.⁵⁸ A previous study shows that EGR1 mediates platelet-derived growth factor-induced sphingosine kinase 1 (SphK1) expression to promote pulmonary artery SMC proliferation.⁵⁹ Recent publications further demonstrate that serine/arginine-rich splicing factor 1 promotes vascular SMC proliferation through an EGR1/KLF5-mediated signaling pathway.⁶⁰ In addition, EGR1 activation is dependent on MEK-ERK signaling.^{31,32} Constitutively bound ELK1 at the EGR1 proximal promoter occurs, which leads to increased pELK1 binding and de novo recruitment of RNA polymerase II to this region.³² In our study, we first focused on a panel of transcription factors predicted to interact with *MIAT* based on an *in silico* analysis. This analysis revealed *ELK1* and *EGR1* as relevant targets. Activation of ERK signaling increased cell proliferation, whereas blocking ERK signaling abolished this phenotype. In line with this concept and previous studies,³⁰ we confirmed that *EGR1* expression was highly increased in advanced carotid plaques and positively correlated with *MIAT* expression and SMC proliferation rates.

Macrophage infiltration and activation around lipid pools is crucial for necrotic core formation and progressing plaque vulnerability.⁶¹ In atherosclerotic lesions, macrophages scavenge oxLDL, which has strong proinflammatory and immunogenic properties.^{62,63} NF- κ B signaling is thought to be involved in this process⁶⁴ and inhibition of NF- κ B prevents foam cell formation and plaque destabilization.⁶⁵ Our current discovery that knockdown of *MIAT* impaired oxLDL uptake in human monocyte-differentiated and murine peritoneal macrophages suggests that *MIAT* regulates inflammation and lesion progression in carotid plaques. Furthermore, oxLDL-induced activation and translocation of NF- κ B were attenuated after inhibiting *MIAT* and blocking its proinflammatory contribution to plaque progression through direct targeting of the NF- κ B subunit NF κ B2/p52/p100.

Conventionally, phenotypic switching of SMCs from quiescent and contractile to proliferative and synthetic states occurs during vascular development and in response to injury.⁶⁶ Recent studies suggest that SMCs that undergo phenotypic switching can acquire macrophage-like properties, which is of fundamental importance to atherosclerosis.⁶⁷ This transdifferentiation process, which plays a key role in plaque pathogenesis, seems to be heavily dependent on KLF4 activity.⁹ Cooperative binding of KLF4, pELK-1, and HDAC2 to a G-C repressor element in the SM22 α promoter mediates this process.⁸ SMC-specific conditional knockout of KLF4 results in reduced numbers of SMC-derived mesenchymal stem cells and macrophage-like cells, and marked reductions in lesion size, as well, and increases in multiple

indices of plaque stability.⁹ Consistent with our results, KLF4, ELK1, and HDAC2 are induced by increased *MIAT* expression or oxLDL stimulation. Elevated *MIAT* levels and oxLDL induction, as well, resulted in reduced expression of SMC markers (ACTA2) and increased macrophage determinants (CD68). The knockdown of *MIAT* reversed these changes, suggesting that *MIAT* is crucially involved in oxLDL-induced SMC-macrophage transdifferentiation through control of KLF4. Our data suggest direct binding of *MIAT* to the *KLF4* promoter, which is sufficient to induce its transcription. *MIAT* is not the only lncRNA with an enhancer-like function. Similar roles have been described previously for *H19* in abdominal aortic aneurysm²⁹ and, more recently, for *REG1CP* in promoting tumorigenesis through *REG3A*.⁶⁸

The effect of experimental *MIAT* modulation appears to be quite complex. *Miat*^{-/-}*ApoE*^{-/-} mice seem largely protected from developing advanced lesions compared with littermate *Miat*^{+/+}*ApoE*^{-/-} controls. During atherosclerosis, genetic depletion of *Miat* limited *Klf4*-mediated SMC-macrophage transition and inflammation. However, once lesions were established in *Miat*^{-/-}*ApoE*^{-/-} animals, they appeared unstable and more likely to rupture than *Miat* wildtype (but *ApoE*^{-/-}) littermate controls in our experimental plaque rupture model. The downregulation of the direct *Miat* targets *Erk*, *Elk1*, and *Egr1* was responsible for the limited SMC proliferation and the resulting fibrous cap thinning.

In conclusion, we identified a key functional role for the lncRNA *MIAT* in atherosclerotic plaque development and destabilization. In high-risk individuals with advanced atherosclerotic plaques, increased *MIAT* expression has 3 main effects after exposure to elevated oxLDL and Lp(a) levels: (1) it can promote SMC proliferation through the ERK-ELK1-EGR1 pathway; (2) it activates proinflammatory macrophages through NF- κ B signaling, and (3) it mediates SMC phenotypic transdifferentiation to inflammatory macrophage-like cells through increasing the transcriptional activity of *KLF4*. Knockdown of *MIAT* in vitro and in vivo mitigated these disease-relevant consequences. Ultimately targeting *MIAT* can serve as a novel molecular treatment strategy to limit vascular inflammation and atherosclerosis progression under certain conditions.

ARTICLE INFORMATION

Received October 7, 2020; accepted September 22, 2021.

Affiliations

Department for Vascular and Endovascular Surgery, Klinikum rechts der Isar, Technical University Munich, Germany (FF, J. Pauli, H.W., N.G., S.B., S.M., Z.W., W.K., H.-H.E., V.P., L. Maegdefessel). German Center for Cardiovascular Research (DZHK), Berlin, Germany; partner site Munich Heart Alliance (FF, J. Pauli, H.W., FF, N.G., S.B., S.M., Z.W., W.K., H.-H.E., V.P., L. Maegdefessel). Department of Medicine (H.J., G.W., E.C., A.B.), Department of Molecular Medicine and Surgery (H.-J., L. Matic, U.H., C.B., L. Maegdefessel), Karolinska Institutet, Stockholm, Sweden. Department of Cardiology, Columbia University Medical Center, New York, NY (D.Y.L., M.R.). Robarts Research Institute, Western University, Ontario, Canada

(M.L.K.). Department of Vascular Surgery, University Hospital Zurich, Switzerland (J. Pelisek). Department of Experimental Pathology, Westphalian Wilhelms University, Munster, Germany (O.S.). Department of Physiology and Pharmacology, Karolinska Institutet, Stockholm, Sweden (O.S.). Institute for Cardiovascular Prevention, Ludwig Maximilian University of Munich, Germany (O.S.).

Acknowledgments

The authors greatly appreciate the *pCAG_Miat* vector that Dr Blackshaw (The Johns Hopkins University, Baltimore, MD) and Prof Qin (University of Alabama at Birmingham) kindly provided. *Miat*-deficient mice (originally denoted *Gomafu* CD-B1347K) were a kind gift from Prof Nakagawa at the RIKEN Center for Life Science Technologies, Kobe, Japan. The authors further thank Prof Engelhardt, Dr Dueck, and Dr Ramanujaran (Institute of Pharmacology and Toxicology, Technical University Munich) for critical discussions and sharing of expertise and equipment, and Prof Misgeld, as well, for providing access to confocal microscopy. All have provided permission to be named in the article.

Sources of Funding

This study is supported by the Swedish Heart-Lung-Foundation (20180680), the Swedish Research Council (Vetenskapsrådet, 2019-01577), the European Research Council (ERC-StG *NORVAS*), a DZHK Junior Research Group (JRG_LM_MRI), the SFB1123 and TRR267 of the German Research Council (DFG), the National Institutes of Health (NIH; 1R01HL150359-01), the Bavarian State Ministry of Health and Care through the research project DigiMed Bayern (all to L. Maegdefessel). Dr Winski has received support from The Committee for Doctoral Education at Karolinska Institutet (CSTP/Research Internship programmes). Dr Matic is the recipient of fellowships and awards from the Swedish Research Council (VR, 2019-02027), Swedish Heart-Lung Foundation (HLF, 20200621, 20200520, 20180244, 201602877, 20180247), Swedish Society for Medical Research (SSMF, P13-0171). Dr Matic also acknowledges funding from Sven and Ebba-Christina Hagberg, Tore Nilsson's, Magnus Bergvall's and Karolinska Institute research (KI Fonder) and doctoral education (KID) foundations. Dr Koschinsky is supported by the Heart and Stroke Foundation of Canada.

Disclosures

None.

Supplemental Materials

- Supplemental Methods
- Figures S1–S10
- Tables S1–S4
- References 69–74

REFERENCES

1. Sadat U, Jaffer FA, van Zandvoort MA, Nicholls SJ, Ribatti D, Gillard JH. Inflammation and neovascularization intertwined in atherosclerosis: imaging of structural and molecular imaging targets. *Circulation*. 2014;130:786–794. doi: 10.1161/CIRCULATIONAHA.114.010369
2. van Lammeren GW, den Ruijter HM, Vrijenhoek JE, van der Laan SW, Velema E, de Vries JP, de Kleijn DP, Vink A, de Borst GJ, Moll FL, et al. Time-dependent changes in atherosclerotic plaque composition in patients undergoing carotid surgery. *Circulation*. 2014;129:2269–2276. doi: 10.1161/CIRCULATIONAHA.113.007603
3. Fernández-Friera L, Peñalvo JL, Fernández-Ortiz A, Ibañez B, López-Melgar B, Laclaustra M, Oliva B, Moco-roa A, Mendiguren J, Martínez de Vega V, et al. Prevalence, vascular distribution, and multiterritorial extent of subclinical atherosclerosis in a middle-aged cohort: the PESA (Progression of Early Subclinical Atherosclerosis) study. *Circulation*. 2015;131:2104–2113. doi: 10.1161/CIRCULATIONAHA.114.014310
4. Donnan GA, Fisher M, Macleod M, Davis SM. Stroke. *Lancet*. 2008;371:1612–1623. doi: 10.1016/S0140-6736(08)60694-7
5. Libby P, Ridker PM, Hansson GK. Progress and challenges in translating the biology of atherosclerosis. *Nature*. 2011;473:317–325. doi: 10.1038/nature10146
6. Chappell J, Harman JL, Narasimhan VM, Yu H, Foote K, Simons BD, Bennett MR, Jørgensen HF. Extensive proliferation of a subset of differentiated, yet plastic, medial vascular smooth muscle cells contributes to neointimal formation in mouse injury and atherosclerosis models. *Circ Res*. 2016;119:1313–1323. doi: 10.1161/CIRCRESAHA.116.309799
7. Cai Y, Nagel DJ, Zhou Q, Cygnar KD, Zhao H, Li F, Pi X, Knight PA, Yan C. Role of cAMP-phosphodiesterase 1C signaling in regulating growth factor receptor stability, vascular smooth muscle cell growth, migra-

- tion, and neointimal hyperplasia. *Circ Res*. 2015;116:1120–1132. doi: 10.1161/CIRCRESAHA.116.304408
8. Salmon M, Gomez D, Greene E, Shankman L, Owens GK. Cooperative binding of KLF4, pELK-1, and HDAC2 to a G/C repressor element in the SM22 α promoter mediates transcriptional silencing during SMC phenotypic switching in vivo. *Circ Res*. 2012;111:685–696. doi: 10.1161/CIRCRESAHA.112.269811
9. Shankman LS, Gomez D, Cherepanova OA, Salmon M, Alencar GF, Haskins RM, Swiatlowska P, Newman AA, Greene ES, Straub AC, et al. KLF4-dependent phenotypic modulation of smooth muscle cells has a key role in atherosclerotic plaque pathogenesis. *Nat Med*. 2015;21:628–637. doi: 10.1038/nm.3866
10. Finney AC, Funk SD, Green JM, Yurdagul A Jr, Rana MA, Pistorius R, Henry M, Yurochko A, Pattillo CB, Traylor JG, et al. EphA2 expression regulates inflammation and fibroproliferative remodeling in atherosclerosis. *Circulation*. 2017;136:566–582. doi: 10.1161/CIRCULATIONAHA.116.026644
11. Zysset D, Weber B, Rihs S, Brasseit J, Freigang S, Riether C, Banz Y, Cerwenka A, Simillion C, Marques-Vidal P, et al. TREM-1 links dyslipidemia to inflammation and lipid deposition in atherosclerosis. *Nat Commun*. 2016;7:13151. doi: 10.1038/ncomms13151
12. Luo Y, Duan H, Qian Y, Feng L, Wu Z, Wang F, Feng J, Yang D, Qin Z, Yan X. Macrophagic CD146 promotes foam cell formation and retention during atherosclerosis. *Cell Res*. 2017;27:352–372. doi: 10.1038/cr.201718
13. Sarrazay V, Sore S, Viaud M, Rignol G, Westerterp M, Ceppo F, Tanti JF, Guinamard R, Gautier EL, Yvan-Charvet L. Maintenance of macrophage redox status by ChREBP limits inflammation and apoptosis and protects against advanced atherosclerotic lesion formation. *Cell Rep*. 2015;13:132–144. doi: 10.1016/j.celrep.2015.08.068
14. Batista PJ, Chang HY. Long noncoding RNAs: cellular address codes in development and disease. *Cell*. 2013;152:1298–1307. doi: 10.1016/j.cell.2013.02.012
15. Cech TR, Steitz JA. The noncoding RNA revolution—trashing old rules to forge new ones. *Cell*. 2014;157:77–94. doi: 10.1016/j.cell.2014.03.008
16. Ishii N, Ozaki K, Sato H, Mizuno H, Susumu Saito, Takahashi A, Miyamoto Y, Ikegawa S, Kamatani N, Hori M, et al. Identification of a novel non-coding RNA, MIAT, that confers risk of myocardial infarction. *J Hum Genet*. 2006;51:1087–1099. doi: 10.1007/s10038-006-0070-9
17. Liu Y, Li L, Su Q, Liu T, Ma Z, Yang H. Ultrasound-targeted microbubble destruction enhances gene expression of microRNA-21 in swine heart via intracoronary delivery. *Echocardiography*. 2015;32:1407–1416. doi: 10.1111/echo.12876
18. Perisic L, Aldi S, Sun Y, Folkersen L, Razuvaev A, Roy J, Lengquist M, Åkesson S, Wheelock CE, Maegdefessel L, et al. Gene expression signatures, pathways and networks in carotid atherosclerosis. *J Intern Med*. 2016;279:293–308. doi: 10.1111/joim.12448
19. Pelisek J, Hegenloh R, Bauer S, Metschl S, Pauli J, Glukha N, Busch A, Reutersberg B, Kallmayer M, Trenner M, et al. Biobanking: objectives, requirements, and future challenges—experiences from the Munich Vascular Biobank. *J Clin Med*. 2019;8:E251. doi: 10.3390/jcm8020251
20. Eken SM, Jin H, Chernogubova E, Li Y, Simon N, Sun C, Korzunowicz G, Busch A, Bäcklund A, Österholm C, et al. MicroRNA-210 enhances fibrous cap stability in advanced atherosclerotic lesions. *Circ Res*. 2017;120:633–644. doi: 10.1161/CIRCRESAHA.116.309318
21. Jin H, Li DY, Chernogubova E, Sun C, Busch A, Eken SM, Saliba-Gustafsson P, Winter H, Winski G, Raaz U, et al. Local delivery of miR-21 stabilizes fibrous caps in vulnerable atherosclerotic lesions. *Mol Ther*. 2018;26:1040–1055. doi: 10.1016/j.yjthe.2018.01.011
22. Zhu XH, Yuan YX, Rao SL, Wang P. LncRNA MIAT enhances cardiac hypertrophy partly through sponging miR-150. *Eur Rev Med Pharmacol Sci*. 2016;20:3653–3660.
23. Shen Y, Dong LF, Zhou RM, Yao J, Song YC, Yang H, Jiang Q, Yan B. Role of long non-coding RNA MIAT in proliferation, apoptosis and migration of lens epithelial cells: a clinical and in vitro study. *J Cell Mol Med*. 2016;20:537–548. doi: 10.1111/jcmm.12755
24. Zhang HY, Zheng FS, Yang W, Lu JB. The long non-coding RNA MIAT regulates zinc finger E-box binding homeobox 1 expression by sponging miR-150 and promoting cell invasion in non-small-cell lung cancer. *Gene*. 2017;633:61–65. doi: 10.1016/j.gene.2017.08.009
25. Hnisz D, Day DS, Young RA. Insulated neighborhoods: structural and functional units of mammalian gene control. *Cell*. 2016;167:1188–1200. doi: 10.1016/j.cell.2016.10.024
26. Levine M, Cattoglio C, Tjian R. Looping back to leap forward: transcription enters a new era. *Cell*. 2014;157:13–25. doi: 10.1016/j.cell.2014.02.009

27. Apostolou E, Hochedlinger K. Chromatin dynamics during cellular reprogramming. *Nature*. 2013;502:462–471. doi: 10.1038/nature12749
28. Chang TH, Huang HY, Hsu JB, Weng SL, Horng JT, Huang HD. An enhanced computational platform for investigating the roles of regulatory RNA and for identifying functional RNA motifs. *BMC Bioinformatics*. 2013;14(suppl 2):S4. doi: 10.1186/1471-2105-14-S2-S4
29. Li DY, Busch A, Jin H, Chernogubova E, Pelisek J, Karlsson J, Sennblad B, Liu S, Lao S, Hofmann P, et al. H19 induces abdominal aortic aneurysm development and progression. *Circulation*. 2018;138:1551–1568. doi: 10.1161/CIRCULATIONAHA.117032184
30. McCaffrey TA, Fu C, Du B, Eksinar S, Kent KC, Bush H Jr, Kreiger K, Rosengart T, Cybulsky MI, Silverman ES, et al. High-level expression of Egr-1 and Egr-1-inducible genes in mouse and human atherosclerosis. *J Clin Invest*. 2000;105:653–662. doi: 10.1172/JCI8592
31. Kamimura M, Viedt C, Dalpke A, Rosenfeld ME, Mackman N, Cohen DM, Blessing E, Preusch M, Weber CM, Kreuzer J, et al. Interleukin-10 suppresses tissue factor expression in lipopolysaccharide-stimulated macrophages via inhibition of Egr-1 and a serum response element/MEK-ERK1/2 pathway. *Circ Res*. 2005;97:305–313. doi: 10.1161/01.RES.0000177893.24574.13
32. Shan J, Balasubramanian MN, Donelan W, Fu L, Hayner J, Lopez MC, Baker HV, Kilberg MS. A mitogen-activated protein kinase/extracellular signal-regulated kinase (MEK)-dependent transcriptional program controls activation of the early growth response 1 (EGR1) gene during amino acid limitation. *J Biol Chem*. 2014;289:24665–24679. doi: 10.1074/jbc.M114.565028
33. Nordestgaard BG, Chapman MJ, Ray K, Borén J, Andreotti F, Watts GF, Ginsberg H, Amarencu P, Catapano A, Descamps OS, et al; European Atherosclerosis Society Consensus Panel. Lipoprotein(a) as a cardiovascular risk factor: current status. *Eur Heart J*. 2010;31:2844–2853. doi: 10.1093/eurheartj/ehq386
34. Cho T, Romagnuolo R, Scipione C, Boffa MB, Koschinsky ML. Apo lipoprotein(a) stimulates nuclear translocation of β -catenin: a novel pathogenic mechanism for lipoprotein(a). *Mol Biol Cell*. 2013;24:210–221. doi: 10.1091/mbc.E12-08-0637
35. Johnson JL, Baker AH, Oka K, Chan L, Newby AC, Jackson CL, George SJ. Suppression of atherosclerotic plaque progression and instability by tissue inhibitor of metalloproteinase-2: involvement of macrophage migration and apoptosis. *Circulation*. 2006;113:2435–2444. doi: 10.1161/CIRCULATIONAHA.106.613281
36. Boffa MB, Koschinsky ML. Oxidized phospholipids as a unifying theory for lipoprotein(a) and cardiovascular disease. *Nat Rev Cardiol*. 2019;16:305–318. doi: 10.1038/s41569-018-0153-2
37. de Vries MR, Ewing MM, de Jong RCM, MacArthur MR, Karper JC, Peters EAB, Nordzell M, Karabina SAP, Sexton D, Dahlbom I, et al. Identification of IgG1 isotype phosphorylcholine antibodies for the treatment of inflammatory cardiovascular diseases. *J Intern Med*. 2021;290:141–156. doi: 10.1111/joim.13234
38. Liu B, Sun L, Liu Q, Gong C, Yao Y, Lv X, Lin L, Yao H, Su F, Li D, et al. A cytoplasmic NF- κ B interacting long noncoding RNA blocks I κ B phosphorylation and suppresses breast cancer metastasis. *Cancer Cell*. 2015;27:370–381. doi: 10.1016/j.ccr.2015.02.004
39. Kawai-Kowase K, Owens GK. Multiple repressor pathways contribute to phenotypic switching of vascular smooth muscle cells. *Am J Physiol Cell Physiol*. 2007;292:C59–C69. doi: 10.1152/ajpcell.00394.2006
40. He S, Zhang H, Liu H, Zhu H. LongTarget: a tool to predict lncRNA DNA-binding motifs and binding sites via Hoogsteen base-pairing analysis. *Bioinformatics*. 2015;31:178–186. doi: 10.1093/bioinformatics/btu643
41. Engreitz JM, Ollikainen N, Guttman M. Long non-coding RNAs: spatial amplifiers that control nuclear structure and gene expression. *Nat Rev Mol Cell Biol*. 2016;17:756–770. doi: 10.1038/nrm.2016.126
42. Wu G, Cai J, Han Y, Chen J, Huang ZP, Chen C, Cai Y, Huang H, Yang Y, Liu Y, et al. LincRNA-p21 regulates neointima formation, vascular smooth muscle cell proliferation, apoptosis, and atherosclerosis by enhancing p53 activity. *Circulation*. 2014;130:1452–1465. doi: 10.1161/CIRCULATIONAHA.114.011675
43. Cho H, Shen GQ, Wang X, Wang F, Archacki S, Li Y, Yu G, Chakrabarti S, Chen Q, Wang QK. Long noncoding RNA ANRIL regulates endothelial cell activities associated with coronary artery disease by up-regulating CLIP1, EZR, and LYVE1 genes. *J Biol Chem*. 2019;294:3881–3898. doi: 10.1074/jbc.RA118.005050
44. Tan P, Guo YH, Zhan JK, Long LM, Xu ML, Ye L, Ma XY, Cui XJ, Wang HQ. LncRNA-ANRIL inhibits cell senescence of vascular smooth muscle cells by regulating miR-181a/Sirt1. *Biochem Cell Biol*. 2019;97:571–580. doi: 10.1139/bcb-2018-0126
45. Lyu Q, Xu S, Lyu Y, Choi M, Christie CK, Slivano OJ, Rahman A, Jin ZG, Long X, Xu Y, et al. SENCR stabilizes vascular endothelial cell adherens junctions through interaction with CKAP4. *Proc Natl Acad Sci USA*. 2019;116:546–555. doi: 10.1073/pnas.1810729116
46. Boulberdaa M, Scott E, Ballantyne M, Garcia R, Descamps B, Angelini GD, Brittan M, Hunter A, McBride M, McClure J, et al. A role for the long noncoding RNA SENCR in commitment and function of endothelial cells. *Mol Ther*. 2016;24:978–990. doi: 10.1038/mt.2016.41
47. Michalik KM, You X, Manavski Y, Doddaballapur A, Zörnig M, Braun T, John D, Ponomareva Y, Chen W, Uchida S, et al. Long noncoding RNA MALAT1 regulates endothelial cell function and vessel growth. *Circ Res*. 2014;114:1389–1397. doi: 10.1161/CIRCRESAHA.114.303265
48. Haemmig S, Yang D, Sun X, Das D, Ghaffari S, Molinaro R, Chen L, Deng Y, Freeman D, Moullan N, et al. Long noncoding RNA SNHG12 integrates a DNA-PK-mediated DNA damage response and vascular senescence. *Sci Transl Med*. 2020;12:eaaaw1868. doi: 10.1126/scitranslmed.aaw1868
49. Uchida S, Dimmeler S. Long noncoding RNAs in cardiovascular diseases. *Circ Res*. 2015;116:737–750. doi: 10.1161/CIRCRESAHA.116.302521
50. Li K, Blum Y, Verma A, Liu Z, Pramanik K, Leigh NR, Chun CZ, Samant GV, Zhao B, Garnaas MK, et al. A noncoding antisense RNA in tie-1 locus regulates tie-1 function in vivo. *Blood*. 2010;115:133–139. doi: 10.1182/blood-2009-09-242180
51. Vacante F, Rodor J, Lalwani MK, Mahmoud AD, Bennett M, De Pace AL, Miller E, Van Kuijk K, de Bruijn J, Gijbels M, et al. CARMN loss regulates smooth muscle cells and accelerates atherosclerosis in mice. *Circ Res*. 2021;128:1258–1275. doi: 10.1161/CIRCRESAHA.120.318688
52. Sone M, Hayashi T, Tarui H, Agata K, Takeichi M, Nakagawa S. The mRNA-like noncoding RNA Gomafu constitutes a novel nuclear domain in a subset of neurons. *J Cell Sci*. 2007;120(pt 15):2498–2506. doi: 10.1242/jcs.009357
53. Rapicavoli NA, Poth EM, Blackshaw S. The long noncoding RNA RNCR2 directs mouse retinal cell specification. *BMC Dev Biol*. 2010;10:49. doi: 10.1186/1471-213X-10-49
54. Zhou X, Zhang W, Jin M, Chen J, Xu W, Kong X. lncRNA MIAT functions as a competing endogenous RNA to upregulate DAPK2 by sponging miR-22-3p in diabetic cardiomyopathy. *Cell Death Dis*. 2017;8:e2929. doi: 10.1038/cddis.2017.321
55. Qu X, Du Y, Shu Y, Gao M, Sun F, Luo S, Yang T, Zhan L, Yuan Y, Chu W, et al. MIAT is a pro-fibrotic long non-coding RNA governing cardiac fibrosis in post-infarct myocardium. *Sci Rep*. 2017;7:42657. doi: 10.1038/srep42657
56. Jiang Q, Shan K, Qun-Wang X, Zhou RM, Yang H, Liu C, Li YJ, Yao J, Li XM, Shen Y, et al. Long non-coding RNA-MIAT promotes neurovascular remodeling in the eye and brain. *Oncotarget*. 2016;7:49688–49698. doi: 10.18632/oncotarget.10434
57. Hippe DS, Phan BAP, Sun J, Isquith DA, O'Brien KD, Crouse JR, Anderson T, Huston J, Marcovina SM, Hatsukami TS, et al. Lp(a) (lipoprotein(a)) levels predict progression of carotid atherosclerosis in subjects with atherosclerotic cardiovascular disease on intensive lipid therapy: an analysis of the AIM-HIGH (Atherothrombosis Intervention in Metabolic Syndrome With Low HDL/High Triglycerides: Impact on Global Health Outcomes) Carotid Magnetic Resonance Imaging Substudy-brief report. *Arterioscler Thromb Vasc Biol*. 2018;38:673–678. doi: 10.1161/ATVBAHA.117.310368
58. Khachigian LM, Lindner V, Williams AJ, Collins T. Egr-1-induced endothelial gene expression: a common theme in vascular injury. *Science*. 1996;271:1427–1431. doi: 10.1126/science.271.5254.1427
59. Sysol JR, Natarajan V, Machado RF. PDGF induces SphK1 expression via Egr-1 to promote pulmonary artery smooth muscle cell proliferation. *Am J Physiol Cell Physiol*. 2016;310:C983–C992. doi: 10.1152/ajpcell.00059.2016
60. Xie N, Chen M, Dai R, Zhang Y, Zhao H, Song Z, Zhang L, Li Z, Feng Y, Gao H, et al. SRSF1 promotes vascular smooth muscle cell proliferation through a Δ 133p53/EGR1/KLF5 pathway. *Nat Commun*. 2017;8:16016. doi: 10.1038/ncomms16016
61. Finn AV, Kolodgie FD, Virmani R. Correlation between carotid intimal/medial thickness and atherosclerosis: a point of view from pathology. *Arterioscler Thromb Vasc Biol*. 2010;30:177–181. doi: 10.1161/ATVBAHA.108.173609
62. Kimmel DW, Dole WP, Cliffl DE. Elucidation of the role of lectin-like oxLDL receptor-1 in the metabolic responses of macrophages to human oxLDL. *J Lipids*. 2017;2017:8479482. doi: 10.1155/2017/8479482
63. Liu Z, Zhu H, Dai X, Wang C, Ding Y, Song P, Zou MH. Macrophage liver kinase B1 inhibits foam cell formation and atherosclerosis. *Circ Res*. 2017. doi: 10.1161/CIRCRESAHA.117.311546
64. Tian H, Yao ST, Yang NN, Ren J, Jiao P, Zhang X, Li DX, Zhang GA, Xia ZF, Qin SC. D4F alleviates macrophage-derived foam cell apoptosis by inhibiting the NF- κ B-dependent Fas/FasL pathway. *Sci Rep*. 2017;7:7333. doi: 10.1038/s41598-017-07656-0

65. Plotkin JD, Elias MG, Dellinger AL, Kopley CL. NF- κ B inhibitors that prevent foam cell formation and atherosclerotic plaque accumulation. *Nanomedicine*. 2017;13:2037–2048. doi: 10.1016/j.nano.2017.04.013
66. Alexander MR, Owens GK. Epigenetic control of smooth muscle cell differentiation and phenotypic switching in vascular development and disease. *Annu Rev Physiol*. 2012;74:13–40. doi: 10.1146/annurev-physiol-012110-142315
67. Bennett MR, Sinha S, Owens GK. Vascular smooth muscle cells in atherosclerosis. *Circ Res*. 2016;118:692–702. doi: 10.1161/CIRCRESAHA.115.306361
68. Yari H, Jin L, Teng L, Wang Y, Wu Y, Liu GZ, Gao W, Liang J, Xi Y, Feng YC, et al. LncRNA REG1CP promotes tumorigenesis through an enhancer complex to recruit FANCD1 helicase for REG3A transcription. *Nat Commun*. 2019;10:5334. doi: 10.1038/s41467-019-13313-z
69. Schmittgen TD, Livak KJ. Analyzing real-time PCR data by the comparative C(T) method. *Nat Protoc*. 2008;3:1101–1108. doi: 10.1038/nprot.2008.73
70. Wang Y, Zhu W, Levy DE. Nuclear and cytoplasmic mRNA quantification by SYBR green based real-time RT-PCR. *Methods*. 2006;39:356–362. doi: 10.1016/j.jymeth.2006.06.010
71. Stary HC, Chandler AB, Dinsmore RE, Fuster V, Glagov S, Insull W Jr, Rosenfeld ME, Schwartz CJ, Wagner WD, Wissler RW. A definition of advanced types of atherosclerotic lesions and a histological classification of atherosclerosis. A report from the Committee on Vascular Lesions of the Council on Arteriosclerosis, American Heart Association. *Circulation*. 1995;92:1355–1374. doi: 10.1161/01.cir.92.5.1355
72. Redgrave JN, Gallagher P, Lovett JK, Rothwell PM. Critical cap thickness and rupture in symptomatic carotid plaques: the oxford plaque study. *Stroke*. 2008;39:1722–1729. doi: 10.1161/STROKEAHA.107.507988
73. Hermansson A, Ketelhuth DF, Strodtz D, Wurm M, Hansson EM, Nicoletti A, Paulsson-Berne G, Hansson GK. Inhibition of T cell response to native low-density lipoprotein reduces atherosclerosis. *J Exp Med*. 2010;207:1081–1093. doi: 10.1084/jem.20092243
74. Magné J, Gustafsson P, Jin H, Maegdefessel L, Hulténby K, Wernerson A, Eriksson P, Franco-Cereceda A, Kovanen PT, Gonçalves I, et al. ATG16L1 expression in carotid atherosclerotic plaques is associated with plaque vulnerability. *Arterioscler Thromb Vasc Biol*. 2015;35:1226–1235. doi: 10.1161/ATVBAHA.114.304840